Bi-Level Optimization Model for the Coordination Between Transmission and Distribution Systems Interacting with Local Energy Markets

Pouria Sheikhahmadi [1], Salah Bahramara [2], Andrea Mazza [3], Gianfranco Chicco [3], and João P. S. Catalão [4,*]

[1] *Dept. Electrical and Computer Eng., University of Kurdistan, Kurdistan, Sanandaj 66131, Iran*
[2] *Department of Electrical Engineering, Sanandaj Branch, Islamic Azad University, Sanandaj, Iran*
[3] *Dipartimento Energia "Galileo Ferraris", Politecnico di Torino, Italy*
[4] *Faculty of Engineering of the University of Porto and INESC TEC, 4200-465 Porto, Portugal*

* *Correspondence: catalao@fe.up.pt*

Abstract

The coordination between distribution system and transmission system operation in the presence of distributed energy resources (DERs) is a new framework that needs appropriate modeling. Moreover, local energy market models are emerging, and there is the need to describe the decision-making occurring in active distribution systems including the distribution company (Disco) and the DER aggregators. This paper investigates the coordination between transmission, distribution, and DER aggregators that interact in a local market model. The individual objectives of the decision-makers are conflicting with each other. For this purpose, a bi-level optimization approach is proposed, in which the operation problem of the Disco and the day-ahead market clearing managed by the wholesale market operator are considered as the upper- and lower-levels problems, respectively. Moreover, to model the uncertainties of output power of renewable energy sources in the Disco's problem, the information gap decision theory is used. The resulting model is a non-linear bi-level problem, which is transformed into a linear single-level one through the exploitation of the Karush-Kuhn-Tucker conditions and the duality theory. To investigate the effectiveness of the model, two case studies are defined in which the IEEE 33-bus and a real 43-bus distribution systems are connected to the RTS 24-bus power system.

Keywords: bi-level approach; distributed energy resources; distribution system; local energy market; transmission system.

1. Introduction

Distributed Energy Resources (DERs) consist of Distributed Generation (DGs), Energy Storages (ESs), and demand-side solutions such as Demand Side Management (DSM) and Demand Response (DR). The DER diffusion has changed the energy balance in transmission and distribution networks. The various types of DER can be managed by DER aggregators to trade energy in local and wholesale markets. Also the roles of the Transmission System Operators (TSOs) and Distribution System Operators (DSOs), and their interactions with the markets, have to be clearly specified. TSOs and DSOs have the responsibility of maintaining secure operation of their networks and have to support

neutral market functioning [1]. As such, they cannot act as energy market operators. Thereby, specific market managers and aggregators have to be in place to manage the energy trading in the interacting electrical systems. According with the indications of many literature contributions, the Distribution Company (Disco) – a separate entity with respect to the DSO – is assumed in the sequel as the market manager at the distribution system level. The provision of further services such as DER flexibility [2] has to be managed by specific actors, such as the aggregator indicated in the Universal Smart Energy Framework [3] or the new Distribution System Platform Provider envisioned by the "Re-forming the Energy Vision" plan [4].

In this context, the evolution of the markets can be largely facilitated by the TSO-DSO coordination, aiming at improving the cost efficiency, sustainability and reliability of the electrical system operation. Therefore, appropriate frameworks are needed to model the coordination between TSO and DSO in the presence of DERs. An example is given by the five schemes developed within the SmartNet project for representing the TSO-DSO coordination in Europe [5].

1.1. Literature review and contributions

The participation of DERs aggregators in the wholesale markets has been investigated in several studies. The decision-making problem of a demand response aggregator as a price-taker player in wholesale energy markets has been modeled using a bi-level optimization approach in [6]. In this model, the decision-making framework of the aggregator has been modeled as the upper-level (UL) problem and the customers' behavior has been modeled as the lower-level (LL) problem. In [7] the optimal charging/discharging of electric vehicles in an electrical vehicle parking lot has been determined through an aggregator, by considering the uncertain behavior of wholesale energy market prices. The strategic behavior of battery energy storage aggregator in wholesale market has been modeled in [8] using a stochastic bidding and offering approach. In these studies [6-8], the DERs aggregators' problems have been modeled in the wholesale energy markets without considering the interaction between the DSO and TSO.

The operation problem of a distribution network in the presence of DERs has been investigated from different viewpoints in the literature. In [9], the operation problem of a Disco that participates in energy and reserve markets has been modeled. In [10, 11], a bi-level optimization approach has been proposed to model the decision-making framework of a Disco and DER aggregators in the real-time market. The operation problem of the Disco has been investigated in the presence of DR programs [12] and ESs [13] by using bargaining-based cooperative and affine arithmetic-based multi-objective optimization approaches, respectively. The operation problem of active distribution systems (ADSs) including Disco and microgrids (MGs) as the UL and LL decision makers has been modeled using interactive game vector ([14], where the Disco is called Distribution Energy Market Operator – DEMO), and Karush-Kuhn-Tucker (KKT) conditions [15, 16]. The interaction between the Disco and the parking lot owner is modeled using a bi-level optimization approach in [17]. The operation

problem of the distribution networks in the presence of DERs and energy hub systems is modeled using a two-level model in [18]. In these models [9-18], the coordination between TSO and DSO has not been modeled. In other words, the Disco participates as a price-taker player in wholesale markets. Conversely, the Disco participates as a price-maker player in wholesale markets where it trades energy with the DERs in [19], however the operation problem of the DSO and its interaction with the TSO is not modeled in this study.

Three approaches have been presented in [20] to model the distribution locational marginal prices without considering coordination between TSO and DSO. A novel real-time active-reactive optimal power flow approach for distribution systems (DSs) in the presence of wind power stations has been proposed in [21]. The coordination between TSO and DSO has been modeled using common TSO-DSO market model in [22] considering electric vehicle aggregators. Different frameworks for coordination between TSO and DSO to provide reserve have been investigated in [23]. The coordination between TSO and DSO for reactive power management has been studied in [24]. For this purpose, a model predictive control and multi-objective optimization approaches have been used. The decision-making framework of ES aggregators in wholesale energy and reserve markets has been addressed in [25], in which the coordination between TSO and DSO has been modeled based on the centralized market model. The DERs are used by the DSO to provide energy and ancillary services for the distribution networks in [26]. The DSO-TSO coordination is modeled in [27] to minimize the power losses of the both networks in the presence of DERs. The authors of [28] formulated the voltage regulation problem of the distribution network using a robust model predictive approach in which the DSO coordinated the reactive output power of renewable energy sources, energy storages, and on-load tap changers to voltage management. An overview of the decision-making frameworks referring to distribution network operation in the presence of DERs and MGs is presented in [29].

The diffusion of *local energy markets* (LEMs) is one of the key aspects of the current evolution of the energy systems towards a more user-centric approach. In a LEM, both technical issues concerning the correct operation of the local network, and market-based issues referring to energy trading, need to be successfully addressed. The LEM described in [30] is based on the interaction with the distribution network and does not consider the transmission system. A local energy trading managed in an agent-based community microgrid is presented in [31]. The coordinator of the LEM is an entity called in different ways in various contributions, for example Smart Energy Service Provider (SESP) in [32], and LEM Operator in [33]. However, in [32] the ownership and management of the SESP is not precisely defined, and can be performed by the DSO, the community members (e.g., associated in cooperative form), or even a third party. The LEM as a decentralized energy market is addressed in [33] by considering RES, loads, flexible demand, hydrogen vehicles and storage, with a number of independent participants. The LEM Operator receives the offers and bids from the players and clears the LEM by maximizing the social welfare, then sending the result to the players. Alternatively, the players may decide to trade energy with the Disco. Further solutions to operate a

LEM include the event-driven LEM illustrated in [34], in which any consumer may trigger the opening of an energy trading market through the Disco whenever its energy is not sufficient, and the event-driven LEM assisted by a retail energy broker introduced in [35]. A cooperation energy management framework is proposed in [36] to model the energy transaction among several MGs through a LEM.

The proposed model in this paper is compared with the related studies in the literature in Table 1. Moreover, the flowchart of modeling the operation problem of DSs in the presence of DERs aggregators and the Disco with/without considering the LEM is illustrated in Figure 1. Although different aspects of the coordination between TSO and DSO have been investigated in the literature, their coordination considering the interactions with a LEM has not been modeled in details yet. In this paper, the LEM model is incorporated into an appropriate decision-making framework for ADSs, in which the Disco can participate in wholesale markets as a price-maker player. Therefore, the coordination between TSO, DSO, Disco and DER aggregators is modeled using the LEM concept as shown in Figure 1. For this purpose, a bi-level optimization approach is proposed, in which the LEM and the wholesale energy markets are modeled as the UL and LL problems. More specifically, in the UL problem, the Disco receives offers from the DER aggregators and clears the LEM by considering the aggregated DER offers, the energy traded with the TSO, and the technical constraints of the distribution system. On the other hand, the clearing process of the wholesale market is modeled as the LL problem. To model the uncertain behavior of RESs, the information gap decision theory (IGDT) approach is adopted, in which the Disco's decisions to trade energy with DERs aggregators and wholesale market depend on the risk-level of the Disco [37].

The main contributions of this paper are as follows:

- Proposing a bi-level optimization approach to model the coordination between TSO, DSO, Disco, and DER aggregators.
- Analyzing the impacts of the various types of DERs on the TSO-DSO coordination.

The rest of this paper is organized as follows. The problem description is presented in Section 2. Section 3 describes the mathematical formulation of the problem. Numerical case studies are analyzed and discussed in Section 4. Section 5 concludes the paper.

Table 1: Comparison of the proposed model with the models found in the literature.

Ref.	Decision makers in DSO-TSO interaction				Markets		Participating in the wholesale markets	
	TSO	DSO	Disco	DERs aggregators	wholesale	local	Price-taker	Price-maker
[6]	-	-	-	✓	✓	-	✓	-
[7]	-	-	-	✓	✓	-	✓	-
[8]	✓	-	-	✓	✓	-	-	✓
[9]	-	✓	✓	✓	✓	-	✓	-
[10]	-	✓	✓	✓	✓	-	✓	-
[11]	-	✓	✓	✓	✓	-	✓	-
[12]	-	-	✓	✓	✓	-	✓	-
[13]	-	✓	✓	✓	✓	-	✓	-
[14]	-	✓	✓	✓	✓	-	✓	-
[15]	-	-	✓	✓	✓	-	✓	-
[16]	-	-	✓	✓	✓	-	✓	-
[17]	-	✓	✓	✓	✓	-	✓	-
[18]	-	✓	✓	✓	✓	-	✓	-
[19]	✓	-	✓	✓	✓	-	-	✓
[20]	-	✓	-	-	-	-	-	-
[21]	-	✓	-	-	-	-	-	-
[22]	✓	✓	-	-	-	-	-	-
[24]	✓	✓	-	-	-	-	-	-
[25]	✓	✓	-	✓	✓	-	✓	-
[26]	-	✓	✓	✓	✓	-	✓	-
[27]	✓	✓	-	-	-	-	-	-
[28]	-	✓	-	-	-	-	-	-
[30]	-	-	-	✓	-	✓	-	-
[31]	-	-	-	✓	-	✓	-	-
[32]	-	✓	-	✓	-	✓	-	-
[33]	-	✓	-	✓	-	✓	-	-
[34]	-	✓	-	✓	-	✓	-	-
[35]	-	✓	-	✓	-	✓	-	-
[36]	-	-	-	✓	-	✓	-	-
This paper	✓	✓	✓	✓	✓	✓	-	✓

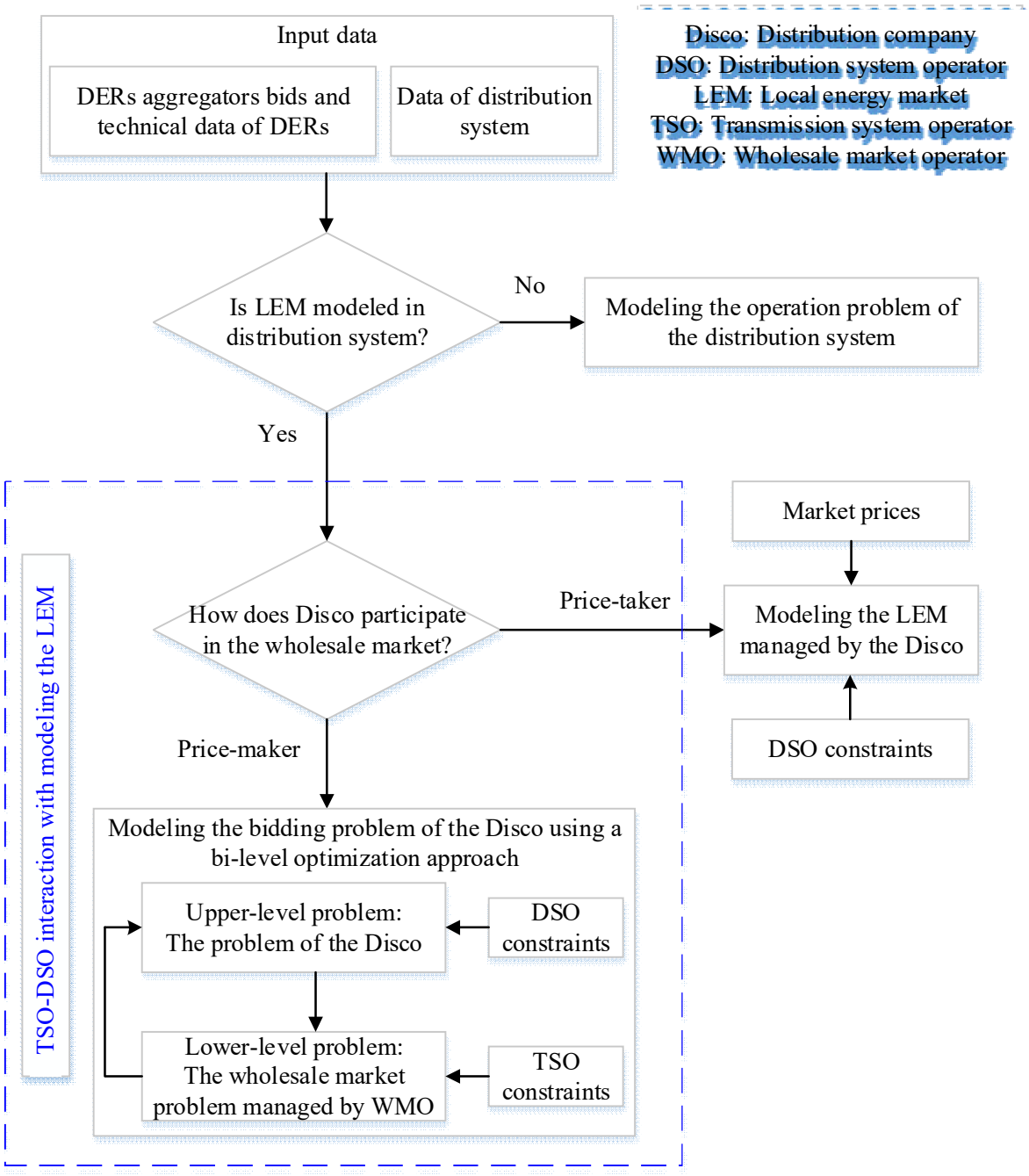

Figure 1. The flowchart of the overall methodology to model the operation problem of the DS with/without LEM considering the DSO-TSO interaction.

2. Problem Description

The decision-making framework addressed in this paper is shown in Figure 2. The proposed framework is mathematically formulated through a bi-level optimization approach (Figure 3). DERs are handled by aggregators consisting of the DG aggregator (DGA), the demand response aggregator (DRA), and renewable energy sources (RESs) aggregator. The DERs aggregators submit their bids and the technical constraints of their DERs to the Disco. Taking into account these data and the technical constraints of the DS, the Disco clears the LEM to meet the require energy demand of the network. For this purpose, the operation problem of the Disco is modeled as a one-stage deterministic

optimization problem (the UL problem). The decision variables of this problem are the bids of the Disco to the wholesale market, the purchased energy from DERs aggregators (the optimal scheduling of DERs), the amount of energy losses, and voltage amplitude at the DS buses.

The Disco participates in the wholesale market to purchase the require energy demand of the DS or to sell its extra energy to this market. The bids of the Disco and the bids/offers of the other market players such as generation companies (Gencos), retailers, and other Discos are sent to the wholesale market operator (WMO). The WMO is a non-profit unit that operates, controls, and manages the wholesale energy market and the ancillary service (AS) markets (reserve and regulation markets) upon TSO requirements. In this paper, the WMO clears the wholesale day-ahead (DA) energy market with the aim of maximizing the social welfare with respect to the technical constraints of the TS (the LL problem). After clearing of the DA market, the power generation of Gencos, the amount of load consumption, power exchanged with the Disco, market clearing prices (*MCP*s), and voltage angles at the TS buses are determined as the decision variables of the LL problem. Considering the amount of the power exchange of the Disco with the wholesale market obtained in the LL problem, the results of the UL problem may change and the new bids for the Disco to participate in the wholesale market are determined. This iterative process is continued until the equilibrium point between the UL and LL problems is obtained. In this paper, this equilibrium point is determined through replacing the proposed non-linear bi-level model into a linear single-level one using the KKT conditions and dual theory. Therefore, the decisions of the Disco in DS and the decisions of the WMO in TS have mutual effects on each other. This shows that the DS dispatching problem depends on the TS operation problem, so that the power losses and the voltage magnitude of the DS depend on the optimal dispatching of the Disco in the DA market.

Moreover, the uncertainties of RES output power is modeled in the decision-making problem of the Disco using the IGDT approach. Regarding the risk-level of the Disco, it manages these uncertainties through changing the decisions to clear the LEM and to trade energy with the wholesale market.

The DERs have the ability to provide the ancillary services (ASs) to the system besides supplying energy for it. For this purpose, five different coordination schemes are proposed in [5]. In each coordination scheme, it is determined in which way the DERs at the distribution level can provide the ASs to the distribution and transmission systems. From these schemes, the local AS market model is compatible with the proposed model in this paper. In this scheme, a separate local market is provided to supply the local requirement to ASs. The DERs aggregators send their offers to the local market where the DSO is the only buyer. The DSO has priority to use local resources for local congestion management. After selection of resources by the DSO, the remaining non-used bids are aggregated by the DSO and transferred to the AS market, operated by the TSO. Since the aim of this paper is to

supply the required energy demand of the system, considering the AS in the proposed coordination model between DSO and TSO is beyond the scope of this paper[1].

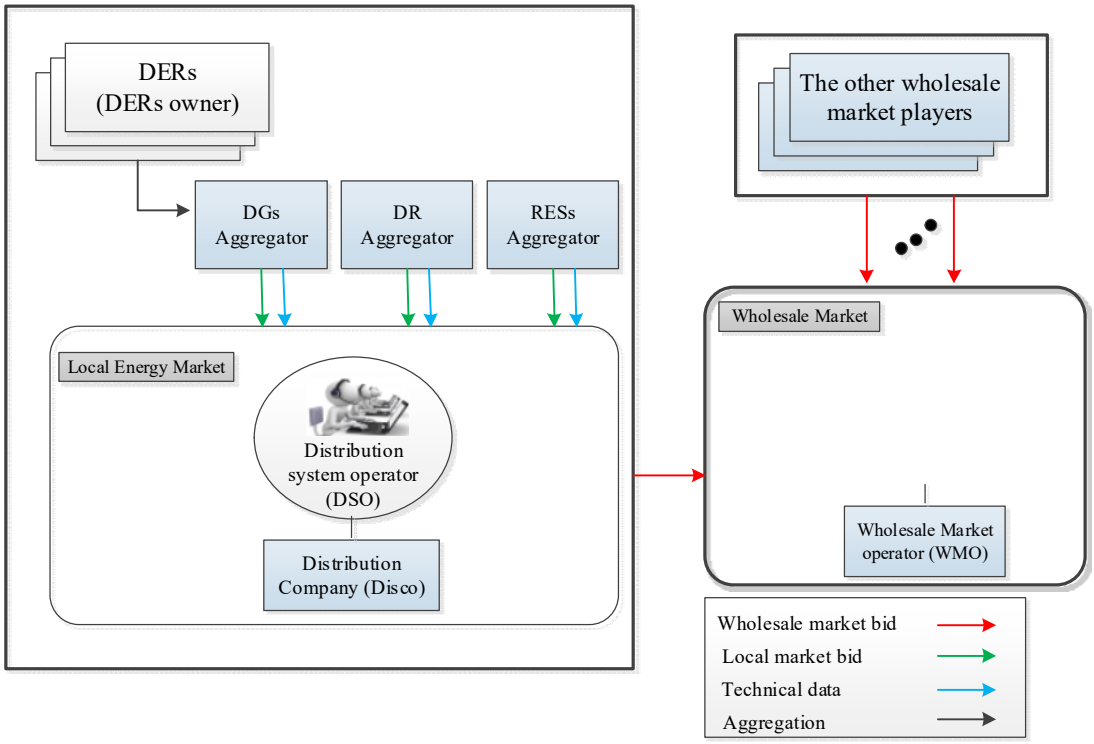

Figure 2. Coordination between TSO, DSO, and DERs aggregators according to local energy market model.

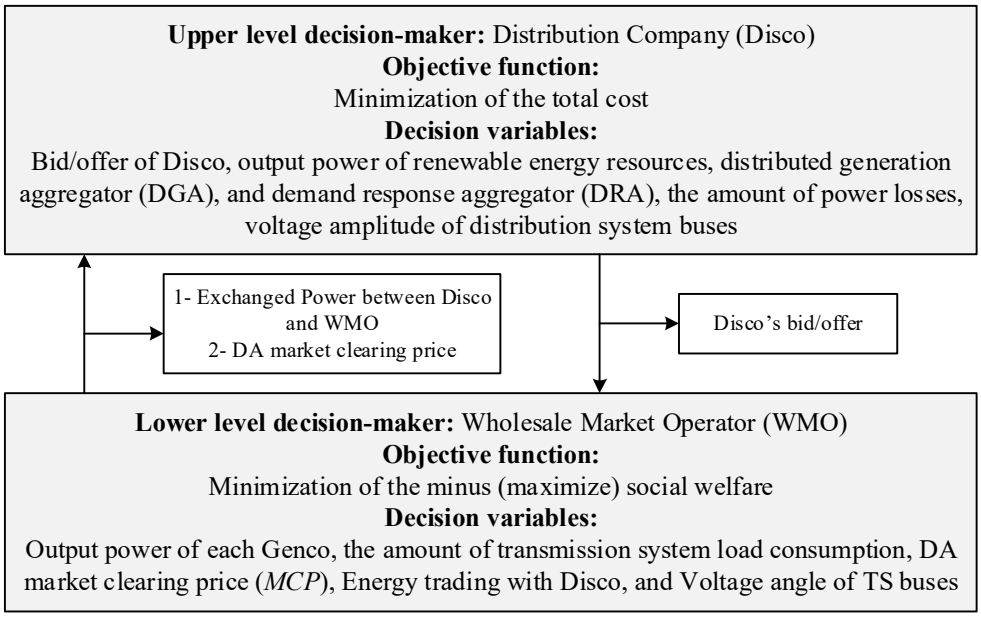

Figure 3. The structure of the proposed bi-level optimization framework.

[1] To develop a local AS market model, the DERs aggregators have to submit their bids to provide AS to the local market. In this case, the local energy and AS markets can be optimized simultaneously, with the Disco participating in both the wholesale energy and AS markets.

3. Mathematical Modeling

The coordination between the transmission and distribution system levels is formulated as a bi-level optimization with the definition of UL and LL problems, as indicated below. The time step considered for the analysis, in which the power values are considered constant, is denoted with d_t.

3.1. Distribution system level with local energy market: UL problem

The UL problem is formulated as follows:

- *Objective function:* The total cost *TC* is minimized as modeled in (1). For each time step considered, the eight terms of the equation correspond to the costs of the following amounts of energy, respectively: taken by the Local Energy System (LES) from the TS, produced from the RES (wind turbines WT and photovoltaic PV), produced from other DG sources, reduced as interruptible load (IL), sold to the distribution system load (DSL) partitioned into responsive load (DSRL) and non-responsive load (DSNL). Furthermore, the load shifting component (SH) is considered for DSRL (see also the constraint (9) below).

$$\text{Min } \{ TC = \sum_{t=1}^{T} \left[\begin{array}{l} \lambda_{m,t}^{\text{TS\_DA}} P_t^{\text{Dis\_DA}} + \sum_{f=1}^{F} C_t^{\text{RES}} P_{f,t}^{\text{WT}} + \sum_{s=1}^{S} C_t^{\text{RES}} P_{s,t}^{\text{PV}} + \sum_{k=1}^{K} \lambda_t^{\text{DG}} P_{k,t}^{\text{DG}} + \\ \sum_{c=1}^{C} (\lambda_t^{\text{IL}} + \lambda_t^{\text{DSL}}) P_{c,t}^{\text{IL}} + \sum_{e=1}^{E} \lambda_t^{\text{SH}} P_{e,t}^{\text{SH}} \Big|_{P_{e,t}^{\text{SH}}>0} - \sum_{e=1}^{E} \lambda_t^{\text{DNL}} P_{e,t}^{\text{DSRL}} \gamma_{e,t} - \sum_{l=1}^{L} \lambda_t^{\text{DSL}} P_{l,t}^{\text{DSNL}} \end{array} \right] \} \quad (1)$$

- *Power balance constraints:* The constraints (2) and (3) guarantee the power balance in the DS reference bus ($i = 1$) and in the other buses ($i \neq 1$), respectively.

$$\sum_{f \in \mathbf{M}_i^{\text{WT}}} P_{f,t}^{\text{WT}} + \sum_{s \in \mathbf{M}_i^{\text{PV}}} P_{s,t}^{\text{PV}} + \sum_{k \in \mathbf{M}_i^{\text{DG}}} P_{k,t}^{\text{DG}} + \sum_{e \in \mathbf{M}_i^{\text{LS}}} \left(1 - \gamma_{e,t}\right) P_{e,t}^{\text{DSRL}} + \sum_{c \in \mathbf{M}_i^{\text{IL}}} P_{c,t}^{\text{IL}} + P_t^{\text{Dis\_DA}} - \sum_{e \in \mathbf{M}_i^{\text{LS}}} P_{e,t}^{\text{DSRL}} - \sum_{l \in \mathbf{M}_i^{\text{NL}}} P_{l,t}^{\text{DSNL}} = 0.5 \left(\sum_{j \in \mathbf{B}_i^{\text{DS}}} P_{i,j,t}^{\text{flow\_DS}} + \sum_{j \in \mathbf{B}_i^{\text{DS}}} P_{i,j,t}^{\text{loss\_DS}} \right) \; : \forall i = 1, \; t \quad (2)$$

$$\sum_{f \in \mathbf{M}_i^{\text{WT}}} P_{f,t}^{\text{WT}} + \sum_{s \in \mathbf{M}_i^{\text{PV}}} P_{s,t}^{\text{PV}} + \sum_{k \in \mathbf{M}_i^{\text{DG}}} P_{k,t}^{\text{DG}} + \sum_{e \in \mathbf{M}_i^{\text{LS}}} \left(1 - \gamma_{e,t}\right) P_{e,t}^{\text{DSRL}} + \sum_{c \in \mathbf{M}_i^{\text{IL}}} P_{c,t}^{\text{IL}} - \sum_{e \in \mathbf{M}_i^{\text{LS}}} P_{e,t}^{\text{DSRL}} - \sum_{l \in \mathbf{M}_i^{\text{NL}}} P_{l,t}^{\text{DSNL}} = 0.5 \left(\sum_{j \in \mathbf{B}_i^{\text{DS}}} P_{i,j,t}^{\text{flow\_DS}} + \sum_{j \in \mathbf{B}_i^{\text{DS}}} P_{i,j,t}^{\text{loss\_DS}} \right) \; : \forall i \neq 1, \; t \quad (3)$$

- *Constraints of RESs:* The constraints (4) and (5) limit the output power of RESs [38].

$$0 \leq P_{f,t}^{\text{WT}} \leq \overline{P}_{f,t}^{\text{WT}} \qquad : \forall f \;, t \quad (4)$$

$$0 \le P_{s,t}^{\mathrm{PV}} \le \overline{P}_{s,t}^{\mathrm{PV}} \quad :\forall s\ ,t \tag{5}$$

- *Constraints of DGA:* The constraints (6) and (7) model the purchased power from DGA and the technical constraints of DGs, such as ramp-down ($\underline{r}$) and ramp-up ($\overline{r}$) limits [9].

$$\underline{P}_{k}^{\mathrm{DG}} u_{k,t}^{\mathrm{DG}} \le P_{k,t}^{\mathrm{DG}} \le \overline{P}_{k}^{\mathrm{DG}} u_{k,t}^{\mathrm{DG}} \quad :\forall k,t \tag{6}$$

$$\underline{r}_{k}^{\mathrm{DG}} \le P_{k,t}^{\mathrm{DG}} - P_{k,\,t-1}^{\mathrm{DG}} \le \overline{r}_{k}^{\mathrm{DG}} \ :\ \forall k,t \tag{7}$$

- *Constraints of DRA:* The constraint (8) limits the upper bound of the ILs provided by DRA. The constraint (9) determines the load shifting (LS) provided by DRA. The LS elasticity rate of the distribution system load (DSL) is limited by (10). The constraint (11) enforces LS between the whole time periods while the total load consumption is considered at a certain level. When $\rho_{\mathrm{LS}} = 1$, this constraint guarantees that the total load consumption across the whole time periods should be unchanged [10].

$$0 \le P_{c,t}^{\mathrm{IL}} \le \overline{P}_{c}^{\mathrm{IL}} \ :\ \forall c\ ,t \tag{8}$$

$$P_{e,t}^{\mathrm{SH}} = \left(1-\gamma_{e,t}\right) P_{e,t}^{\mathrm{DSRL}} \quad :\forall e,t \tag{9}$$

$$0 \le \gamma_{e,t} \le \Gamma_{\mathrm{LS}} \quad :\forall e,t \tag{10}$$

$$\sum_{t}^{T} P_{e,t}^{\mathrm{DSRL}} \gamma_{e,t} = \rho_{\mathrm{LS}} \sum_{t}^{T} P_{e,t}^{\mathrm{DSRL}} \quad :\forall e \tag{11}$$

- *DS power flow constraints:* The aim of the power flow is determining the angle and the magnitude of the node voltages, and to calculate the active and reactive power flows. The model proposed in this paper uses the hypothesis of neglecting the voltage angle, and exploits the linearized power flow equations proposed in [39]. The constraint (12) indicates the difference of the active power flow that leaves node *i* to node *j* and the active power flow that leaves node *j* to node *i*, at time step *t*. The constraint (13) represents the amount of DS active power losses. The constraint (14) defines the amount of current flows from bus *i* to bus *j*. The amount of current from bus i to bus j is limited by (15). The constraint (16) shows the upper and lower bounds of voltage amplitude of DS buses.

$$P_{i,j,t}^{\mathrm{flow\_DS}} = \left(\frac{R_{i,j}^{\mathrm{DS}}}{\left(Z_{i,j}^{\mathrm{DS}}\right)^2} \right) \left(V_{i,t}^{\mathrm{DS\_sqr}} - V_{j,t}^{\mathrm{DS\_sqr}} \right) \quad :\forall i,j,t \tag{12}$$

$$P_{i,j,t}^{\mathrm{loss\_DS}} = R_{i,j}^{\mathrm{DS}} I_{i,j,t}^{\mathrm{DS\_sqr}} \quad :\forall i,j,t \tag{13}$$

$$I_{i,j,t}^{\mathrm{DS}}=\frac{V_{i,t}^{\mathrm{DS}}-V_{j,t}^{\mathrm{DS}}}{Z_{i,j}^{\mathrm{DS}}} \quad :\forall i,j,t \tag{14}$$

$$-\overline{I}_{i,j}^{\mathrm{DS}} \le I_{i,j,t}^{\mathrm{DS}} \le \overline{I}_{i,j}^{\mathrm{DS}} \quad :\forall i,j,t \tag{15}$$

$$\underline{V}^{\mathrm{DS}} \le V_{i,t}^{\mathrm{DS}} \le \overline{V}^{\mathrm{DS}} \quad :\forall i,t \tag{16}$$

The variable array of the UL problem is described as:

$$\Xi_{\mathrm{UL}}=\left\{\begin{matrix} P_{f,t}^{\mathrm{WT}}, P_{s,t}^{\mathrm{PV}}, P_{k,t}^{\mathrm{DG}}, u_{k,t}^{\mathrm{DG}}, P_{c,t}^{\mathrm{IL}}, \gamma_{e,t}, V_{i,t}^{\mathrm{DS}}, V_{i,t}^{\mathrm{DS\_sqr}}, \\ I_{i,j,t}^{\mathrm{DS}}, I_{i,j,t}^{\mathrm{DS\_sqr}}, P_{i,j,t}^{\mathrm{flow\_DS}}, C_{t}^{\mathrm{Dis\_DA}} \end{matrix}\right\}.$$

3.2. DA energy market formulation: LL problem

The LL problem formulation is presented as follows [40]:

- *Objective function:* The objective function of the LL problem is to maximize the social welfare of the DA market modeled by (17). The DA market includes the operation cost of Gencos, the revenue from selling energy to the transmission system loads (TSLs), and the revenue from trading energy with the Disco (a non-negative P_t^{Dis} is a bid, and a negative one is an offer).

$$\mathrm{Min} \sum_{t=1}^{T} d_t \left[\sum_{g=1}^{G}\sum_{b=1}^{B} C_{b,g,t}^{\mathrm{TS\_DA}} \rho_{b,g,t}^{\mathrm{TS}} - \sum_{d=1}^{D}\sum_{b=1}^{B} C_{b,d,t}^{\mathrm{TS\_DA}} l_{b,d,t}^{\mathrm{TS}} - C_t^{\mathrm{Dis\_DA}} P_t^{\mathrm{Dis\_DA}} \right] \tag{17}$$

- *Power balance constraints:* The constraints (18)-(19) guarantee the power balance at DS location bus *m* (equation (18)) and other TS buses (equation (19)).

$$\sum_{g\in \mathbf{M}_n^{\mathrm{G}}} P_{g,t}^{\mathrm{TS}} - P_t^{\mathrm{Dis\_DA}} = \sum_{r\in \mathbf{B}_n^{\mathrm{TS}}} B_{m,r}\left(\theta_{m,t}^{\mathrm{TS\_DA}} - \theta_{r,t}^{\mathrm{TS\_DA}}\right) : \lambda_{n,t}^{\mathrm{TS\_DA}} \quad \forall n=m, \forall t \tag{18}$$

$$\sum_{g\in \mathbf{M}_n^{\mathrm{G}}} P_{g,t}^{\mathrm{TS}} - \sum_{d\in \mathbf{M}_n^{D}} L_{d,t}^{\mathrm{TS}} = \sum_{r\in \mathbf{B}_n^{\mathrm{TS}}} B_{n,r}\left(\theta_{n,t}^{\mathrm{TS\_DA}} - \theta_{r,t}^{\mathrm{TS\_DA}}\right) : \lambda_{n,t}^{\mathrm{TS\_DA}} \quad \forall n\neq m, \forall t \tag{19}$$

- *Constraints of Disco:* The constraint (20) determines the trading limits of the Disco with the market.

$$\underline{P}^{\text{Dis-TS}} \le P_t^{\text{Dis-DA}} \le \overline{P}^{\text{Dis-TS}} : \underline{\mu}_t^{\mathrm{l\_DA}}, \overline{\mu}_t^{\mathrm{l\_DA}} \qquad \forall t \tag{20}$$

- *Constraints of Gencos:* The constraint (21) limits Gencos generation. The constraint (22) limits the upper bounds of energy blocks related to Gencos. The constraint (23) reveals that the summation of energy blocks related to each Genco equals the total Genco output power quantity.

$$\underline{P}_g \le P_{g,t}^{\mathrm{TS}} \le \overline{P_g} \;:\underline{\mu}_{g,t}^{2\_\mathrm{DA}} ,\overline{\mu}_{b,g,t}^{2\_\mathrm{DA}} \quad \forall g ,t \tag{21}$$

$$0 \le \rho_{b,g,t}^{\mathrm{TS}} \le \overline{\rho}_{b,g,t}^{\mathrm{TS}} \;:\underline{\mu}_{b,g,t}^{3\_\mathrm{DA}} ,\overline{\mu}_{b,g,t}^{3\_\mathrm{DA}} \quad \forall b ,g ,t \tag{22}$$

$$\sum_{b=1}^{B} \rho_{b,g,t}^{\mathrm{TS}} = P_{g,t}^{\mathrm{TS}} \;:\lambda_{g,t}^{1\_\mathrm{DA}} \quad \forall g ,t \tag{23}$$

- *Constraints of TSLs:* The constraint (24) limits the TSL consumption. The constraint (25) limits the upper bounds of energy blocks related to TSLs. The constraint (26) indicates that the summation of energy blocks related to each TSL equals the total TSL output power quantity.

$$0 \le L_{d,t}^{\mathrm{TS}} \le \overline{L}_{d,t}^{\mathrm{TS}} \;:\underline{\mu}_{d,t}^{4\_\mathrm{DA}} ,\overline{\mu}_{b,d,t}^{4\_\mathrm{DA}} \quad \forall d ,t \tag{24}$$

$$0 \le l_{b,d,t}^{\mathrm{TS}} \le \overline{l}_{b,d,t}^{\mathrm{TS}} \;:\underline{\mu}_{b,d,t}^{5\_\mathrm{DA}} ,\overline{\mu}_{b,d,t}^{5\_\mathrm{DA}} \quad \forall b ,d ,t \tag{25}$$

$$\sum_{b=1}^{B} l_{b,d,t}^{\mathrm{TS}} = L_{d,t}^{\mathrm{TS}} \;:\lambda_{d,t}^{2\_\mathrm{DA}} \quad \forall d ,t \tag{26}$$

- *Transmission system constraints:* The constraint (27) indicates the capacity limit of the TS line (n, r). The constraint (28) describes the range of TS voltage angles, and the constraint (29) sets the TS slack bus as the angle reference bus.

$$-\overline{f}_{n,r}^{\mathrm{TS}} \le B_{n,r}\left(\theta_{n,t}^{\mathrm{TS\_DA}} - \theta_{r,t}^{\mathrm{TS\_DA}}\right) \le \overline{f}_{n,r}^{\mathrm{TS}} \;:\underline{\mu}_{n,r,t}^{6\_\mathrm{DA}} ,\overline{\mu}_{n,r,t}^{6\_\mathrm{DA}} \;\forall n ,r ,t \tag{27}$$

$$-\frac{\pi}{2} \le \theta_{n,t}^{\mathrm{TS\_DA}} \le \frac{\pi}{2} \;:\underline{\mu}_{n,t}^{7\_\mathrm{DA}} ,\overline{\mu}_{n,t}^{7\_\mathrm{DA}} \quad \forall n ,t \tag{28}$$

$$\theta_{n,t}^{\mathrm{TS\_DA}} = 0 \;:\lambda_{n,t}^{3\_\mathrm{DA}} ,\forall n = slack ,t \tag{29}$$

The array of variables for this problem is $\Xi_{\mathrm{LL}} = \{P_{g,t}^{\mathrm{TS}}, L_{d,t}^{\mathrm{TS}}, \rho_{b,g,t}^{\mathrm{TS}}, l_{b,d,t}^{\mathrm{TS}}, P_t^{\mathrm{Dis\_DA}}, \theta_{n,t}^{\mathrm{TS\_DA}}\}$. Note that the dual variables (Lagrangian multipliers) for each constraint of the LL problem are considered at the right hand side of the formulation.

3.3. Mixed-Integer Linear Programming (MILP)

The model proposed in this paper corresponds to a non-linear bi-level optimization problem, which is transformed into a single-level problem by using the KKT conditions as described in Appendix A. The resulting single-level model is a non-linear problem due to two variables multiplied in its objective function ($\lambda_{m,t}^{\mathrm{TS\_DA}} P_t^{\mathrm{Dis\_DA}}$). This term is then linearized by using the approach presented in Appendix B. The final linear single-level model is presented as follows:

$$\text{Min}\left[\begin{array}{l}\sum_{t=1}^{T} d_t\left[\sum_{g=1}^{G}\sum_{b=1}^{B} C_{b,g,t}^{\text{TS\_DA}}\rho_{b,g,t}^{\text{TS}}-\sum_{d=1}^{D}\sum_{b=1}^{B} C_{b,d,t}^{\text{TS\_DA}} l_{b,d,t}^{\text{TS}}\right]- \\ \sum_{t=1}^{T}\left[\begin{array}{l}\sum_{g=1}^{G}\left(\underline{P_g}\,\underline{\mu}_{g,t}^{2\_\text{DA}}-\overline{P}_g\,\overline{\mu}_{g,t}^{2\_\text{DA}}\right)-\sum_{g=1}^{G}\sum_{b=1}^{B}\overline{\rho}_{b,g,t}^{\text{TS}}\,\overline{\mu}_{b,g,t}^{3\_\text{DA}}-\sum_{d=1}^{D}\overline{L}_{d,t}^{\text{TS}}\,\overline{\mu}_{d,t}^{4\_\text{DA}} \\ -\sum_{d=1}^{D}\sum_{b=1}^{B}\overline{l}_{b,d,t}^{\text{TS}}\,\overline{\mu}_{b,d,t}^{5\_\text{DA}}-\sum_{n=1}^{N}\sum_{r=1}^{R}\left(\overline{f}_{n,r}^{\text{TS}}\,\underline{\mu}_{n,r,t}^{6\_\text{DA}}+\overline{f}_{n,r}^{\text{TS}}\,\overline{\mu}_{n,r,t}^{6\_\text{DA}}\right)-\sum_{n=1}^{N}\left(\underline{\mu}_{n,t}^{7\_\text{DA}}+\overline{\mu}_{n,t}^{7\_\text{DA}}\right)\frac{\pi}{2}\end{array}\right]+ \\ \sum_{t=1}^{T}\left[\begin{array}{l}\sum_{f=1}^{F} C_t^{\text{RES}} P_{f,t}^{\text{WT}}+\sum_{s=1}^{S} C_t^{\text{RES}} P_{s,t}^{\text{PV}}+\sum_{k=1}^{K}\lambda_t^{\text{DG}} P_{k,t}^{\text{DG}}+\sum_{c=1}^{C}(\lambda_t^{\text{IL}}+\lambda_t^{\text{DSL}})P_{c,t}^{\text{IL}}+ \\ \sum_{e=1}^{E}\lambda_t^{\text{SH}} P_{e,t}^{\text{SH}}\Big|_{P_{e,t}^{\text{SH}}>0}-\sum_{e=1}^{E}\lambda_t^{\text{DSL}} P_{e,t}^{\text{DSRL}}\gamma_{e,t}-\sum_{l=1}^{L}\lambda_t^{\text{DSL}} P_{l,t}^{\text{DSNL}}\end{array}\right]\end{array}\right] \quad (30)$$

subject to:

UL constraints: equations (2)-(16)

LL constraints: equations (18), (19), (23), (26), (29), (A.1)-(A.7), and (A.8)-(A.16).

3.4. IGDT-Based optimization model

In this paper, the IGDT approach is employed to model the RESs' uncertainties. For this purpose, firstly, the IGDT background is introduced considering in the formulation which is the problem of the Disco where the RESs uncertainties have to be addressed.

- IGDT Background:

The optimization problems are generally described as follows [41]:

$$f^*(\boldsymbol{\psi},\gamma)=\min\{f(\boldsymbol{\psi},\gamma)\} \quad (31)$$

$$\mathbf{h}(\boldsymbol{\psi},\gamma)=\mathbf{0}\,,\mathbf{g}(\boldsymbol{\psi},\gamma)\le\mathbf{0} \quad (32)$$

$$\gamma\in\mathbb{Y} \quad (33)$$

where γ is the uncertain parameter, $\mathbb{Y}$ is the set of uncertain parameters, and $\boldsymbol{\psi}$ is the array of decision variables. The uncertainty on the parameter γ is defined as (34).

$$\mathcal{U}(\bar{\gamma},\alpha)=\left\{\gamma:\left|\frac{\gamma-\bar{\gamma}}{\bar{\gamma}}\right|\le\alpha\right\},\alpha\ge 0 \quad (34)$$

where $\bar{\gamma}$ is the amount of forecast value of uncertain parameter, and α is the maximum deviation of the uncertain parameter from its forecast value, which it is called as the uncertainty radius. A usual

strategy, which is known as the base model, considers the uncertain parameter equal to its forecast value as follows.

$$f_b^*(\boldsymbol{\psi}, \bar{\gamma}) = \min\{f(\boldsymbol{\psi}, \bar{\gamma})\} \quad (35)$$

$$\mathbf{h}(\boldsymbol{\psi}, \bar{\gamma}) = \mathbf{0}\,, \mathbf{g}(\boldsymbol{\psi}, \bar{\gamma}) \leq \mathbf{0} \quad (36)$$

When the uncertain parameter value is different from its forecast value, the decision maker has to handle with some challenges in making a decision. To model this case, the risk-averse strategy is defined for the decision makers. This strategy is related to a situation that the uncertain parameter may have undesirable effect on the objective function, so that it increases the amount of the objective function in the minimization problems. In this strategy, the maximum uncertainty radius is determined to make the objective function robust against the deviation of uncertain parameters. It is mathematically formulated as (37)-(40) [37].

$$\max\ \{\alpha\} \quad (37)$$

$$\mathbf{h}(\boldsymbol{\psi}, \bar{\gamma}) = \mathbf{0}\,, \mathbf{g}(\boldsymbol{\psi}, \bar{\gamma}) \leq \mathbf{0} \quad (38)$$

$$f(\boldsymbol{\psi}, \gamma) \leq f_b^*(\boldsymbol{\psi}, \bar{\gamma})(1 + \zeta), \quad 0 \leq \zeta \leq 1 \quad (39)$$

$$\gamma = (1 - \alpha)\,\bar{\gamma} \quad (40)$$

- The risk-averse strategy of the Disco

In this paper, the risk-averse strategy is used to model the uncertainties of the output power of RESs in the decision-making problem of the Disco. This strategy is formulated as Eqs. (41)-(44) where the amount of RES output power considering their respective uncertainties is calculated as Eq. (44).

$$\max\ \{\alpha\} \quad (41)$$

$$TC_b = \{TC: \text{minimize } TC\} \quad (42)$$

$$TC \leq\ TC_b(1 + \zeta), \quad 0 \leq \zeta \leq 1 \quad (43)$$

$$0 \leq P_t^{\text{RES}} \leq (1 - \alpha)\,\bar{P}_t^{\text{RES}}, \ \ \bar{P}_t^{\text{RES}} =\ \bar{P}_t^{\mathbf{WT}} +\ \bar{P}_t^{\text{PV}} \quad (44)$$

subject to:

UL constraints: equations (2)-(3)-(6)-(16)

LL constraints: equations (18), (19), (23), (26), (29), (A.1)-(A.7), and (A.8)-(A.16).

4. Numerical Results

To investigate the effectiveness of the proposed model, it is applied on the IEEE 33-bus test system connected to the IEEE 24-bus power system named as Case I. Moreover, to show the ability of the proposed model for the real networks, a 43-bus real DS associated with Kurdistan Province Electricity Distribution Company (KPEDC) in Iran is connected to the same power system network as Case II. The results of both cases are presented in the first and the second following sub-sections. Then, the decisions of the risk-averse Disco to manage the uncertainties of RESs using the IGDT approach is presented in the third sub-section. It should be noted that, the proposed MILP model is solved for the both case studies via the CPLEX12 solver under GAMS 24.1.2, running on a 2.8-GHz Core i5 computer with 6GB RAM. The statistical characteristics of the proposed model as well as the computational time in both case studies are given in Table 2.

Table 2. The characteristics of the proposed model imposed on two types of DS.

Test systems	# Single equations	# Single variables	# Discrete variables	Solution time (s)
Case I	265503	139868	12432	401.34
Case II	327525	171712	12432	598.50

4.1. Case I

4.1.1. Input data

The IEEE 33-bus is considered as the DS test system, with technical data presented in [9, 11]. The other DS data are illustrated in Table 3. Also, the DS is connected to the IEEE 24-bus power system as shown in Figure 4. There are 4 wind turbines (WTs) and 4 photovoltaic (PV) arrays in the DS. The forecast output power of the RESs and DSL and the offers of the aggregators are given in [10]. The technical characteristics of DGs and responsive loads are shown in Table 4. The maximum capacity of the DS power exchange with the market is 60 MW. The TS load number 17 which is located at TS bus 20 (m=20) is replaced with DS. Also, TS bus number 13 is considered as the reference bus. The technical data of each Genco are presented in Table 5. Four blocks are used to model the size of energy and offer costs of Gencos in the DA market [40]. The total amount of energy consumption of each TSL presented in [40] is shared into three blocks of equal size with the three respective bid blocks given in Table 6. All the data of this power system are taken from [40, 42].

Table 3. Technical data and DER locations in Case I.

$\bar{P}_{i,j,t}^{\text{flow\_DS}}$ (MW)	$\underline{P}_{i,j,t}^{\text{flow\_DS}}$ (MW)	$\bar{V}_{i,t}^{\text{DS}}$ (p.u.)	$\underline{V}_{i,t}^{\text{DS}}$ (p.u.)	$V_{\text{base}}^{\text{DS}}$ (kV)	Main substation (MVA)
60	-60	1.1	0.9	12.66	80
Type of DER	WT	PV	DG	IL	LS
DS bus location	12, 18, 21, 33	3, 8, 22, 25	18, 24, 29, 33	8, 24, 25, 30, 31, 32	15-33

Table 4. Characteristics of DGs and responsive loads.

# DG	$\bar{P}_k^{\text{DG}}$ (MW)	$\underline{P}_k^{\text{DG}}$ (MW)	$\overline{r}_k^{\text{DG}}$ (MW/h)	$\underline{r}_k^{\text{DG}}$ (MW/h)	$P_{\text{DG}}^{\text{ini}}$ (MW)
1 , 4	2	0.5	1.5	1.5	0.5
2 , 3	2	0.5	2	2	0
P_t^{DNRL} (% of P_t^{DNL})			$\bar{P}_{\text{IL}}$ (MW)	Γ_{LS}	ρ_{LS}
67			8	1.2	1

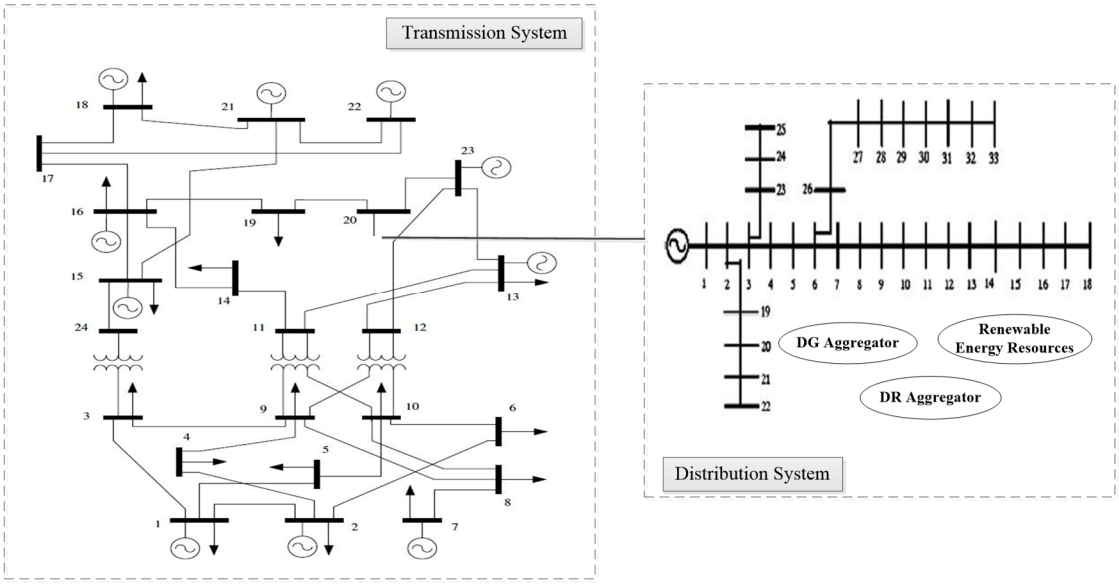

Figure 4. The structure of the 33-bus test DS connected to the 24-bus TS (Case I).

Table 5. Technical data of generator units.

# Genco	$\overline{P_g}$ (MW)	$\underline{P_g}$ (MW)	Node location	# Genco	$\overline{P_g}$ (MW)	$\underline{P_g}$ (MW)	Node location
1	152	0	1	7	155	0	16
2	152	0	2	8	400	0	18
3	350	0	7	9	400	0	21
4	591	0	13	10	300	0	22
5	60	0	15	11	310	0	23
6	155	0	15	12	350	0	23

Table 6. Bids submitted by TSLs.

# TSL	$C_{b,d,t}^{TS}$ ($/MWh)			# TSL	$C_{b,d,t}^{TS}$ ($/MWh)		
	Block 1	Block 2	Block 3		Block 1	Block 2	Block 3
1	39.00	36.40	33.80	9	39.00	36.40	33.80
2	44.20	41.60	39.00	10	44.20	41.60	39.00
3	26.00	20.80	18.20	11	39.00	36.40	33.80
4	39.00	36.40	33.80	12	44.20	41.60	39.00
5	44.20	41.60	39.00	13	26.00	20.80	18.20
6	39.00	36.40	33.80	14	39.00	36.40	33.80
7	44.20	41.60	39.00	15	44.20	41.60	39.00
8	26.00	20.80	18.20	16	39.00	36.40	33.80

4.1.2. Results

The operation costs of the Disco consist of the purchased power from the aggregators and DA market and also, the revenue from power sold to the DSLs are illustrated in Table 7. Moreover, the *MCP*, the power balance between power generation and consumption in the UL and LL problems, the role of the Disco in the DA market as a price-maker player, the sensitivity of the *TC* to the maximum LS factor, and the amount of voltage amplitude at each DS bus are represented in Figures 5-9. It can be noted that only LS is considered for DRA. The amount of active power losses with respect to various types of DERs is illustrated in Table 8.

Table 7. Operation Costs/Revenue of the Disco ($).

Operation cost of RESs	Cost of purchased power from DGA	Cost of purchased power from DRA	Cost of purchased power from market	Revenue from sold power to DSLs	Total cost
903.68	1728.00	380.51	11384.42	-32184.35	-17790.65

As shown in Figures 5 and 6, the *MCP* of the DA market is determined after market clearing process with the aim of maximize social welfare and also, with respect to constraint of the power system, and bids/offers of each market players such as the Gencos, TSLs and Disco. In this market, the Disco acts as a price-maker player at hours 15, 16, 18, 19, 22, and 23. The TSLs determines the *MCP*s at hours 9-14, 17, 20. Also, the Gencos are price-makers at the other time steps.

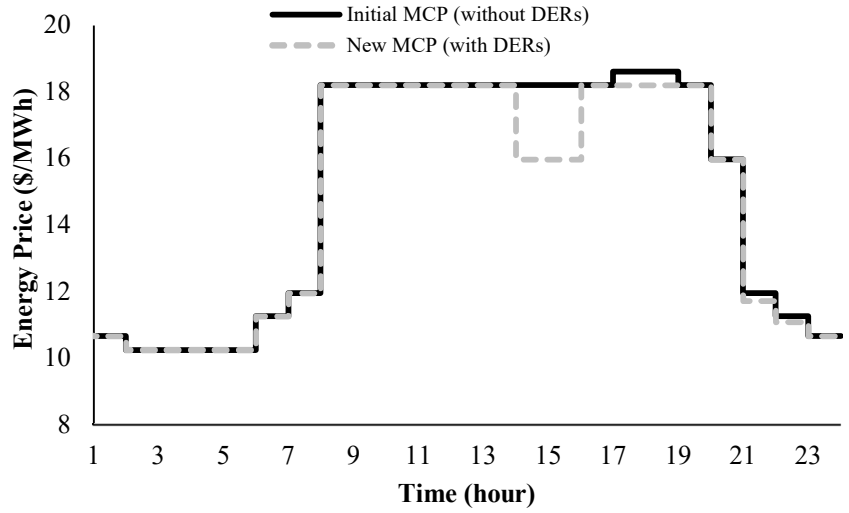

Figure 5. The *MCP* of the DA energy market in Case I.

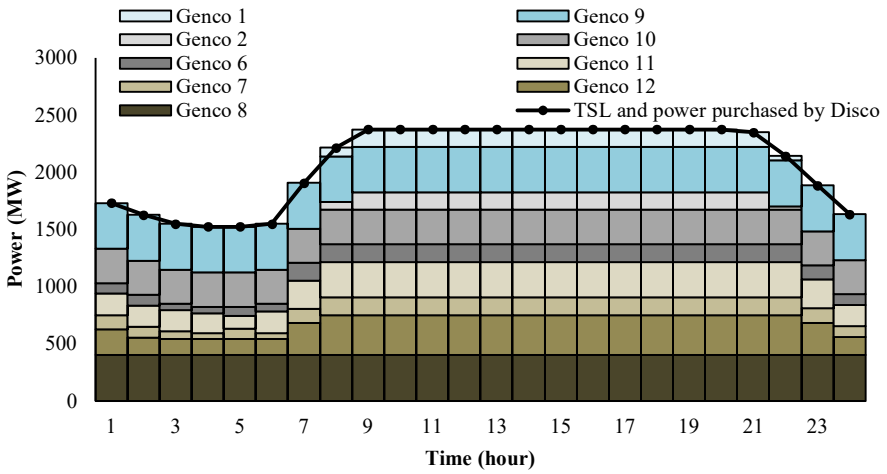

Figure 6. Share of each Genco to meet TSLs and DSL in Case I.

As shown in Figure 7, the Disco decreases the purchased power from the market through optimal scheduling of RESs and optimal trading energy with aggregators. This makes the Disco submitting bids in the DA market at hours with high power delivery in the power system. The bid of the Disco depends on the bids of the DERs aggregator and the technical constraints of the DERs. Therefore, this Disco's action makes the *MCP* decrease at hours 15, 16, 18, and 19 from 18.2, 18.2, 18.6, and 18.6 $/MWh to 15.97, 15.97, 18.2, and 18.2 $/MWh.

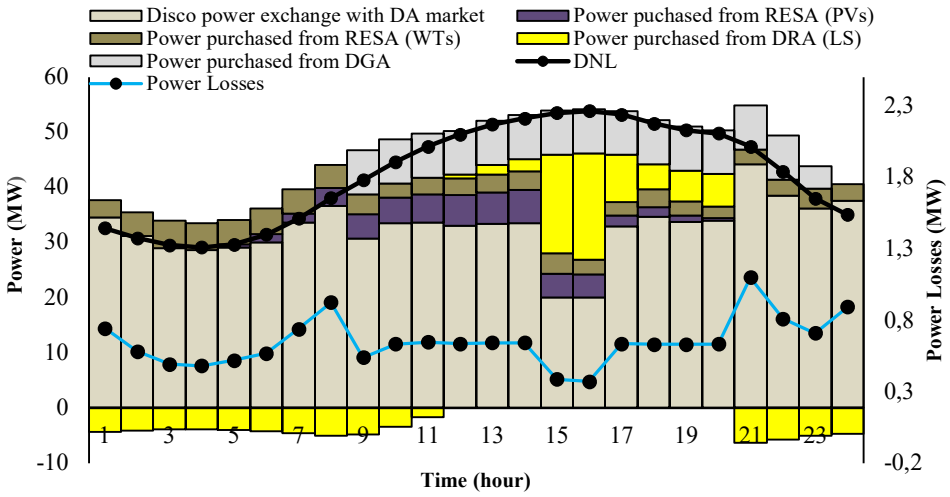

Figure 7. The share of the resources to meet the power balance of the DS in Case I.

On the other hand, the amount of power losses shown in Figure 7 depends on the Disco's decisions to schedule the DERs and to participate as a price-maker player in the DA market. The incorporation of the DS in the calculations is important because of the non-negligible role of the losses in the distribution system that lead to different results with respect to the case without considering the structure of the DS (one-bus DS). For instance, at hours 22 and 23, the Disco decreases the purchased power from the DA market from 45.645 and 39.402 MW to 38.499 and 36.103 MW, respectively. Also, the Disco prefers to increase the purchased power from the aggregators and the power losses decrease in these hours. These Disco's decisions decrease the *MCP*s from 11.96 and 11.26 $/MWh to 11.72 and 11.09 $/MWh.

As mentioned, the types and dynamic behavior of DERs change the Disco's decisions and the amount of power losses at each time steps. For this purpose, it is assumed that the DRA only has ILs. The Disco changes the *MCP*s from 10.66, 18.6, 18.6, and 11.26 $/MWh to 10.25, 18.2, 18.2, and 11.09 $/MWh at hours 2, 18, 19, and 23 using interaction with the DERs and also, the Disco decreases the *MCP* from 10.66 $/MWh to 10.25 $/MWh at hour 24 due to considering the ILs and their impact on the power losses.

The voltage amplitude of the DS buses with/without considering the DERs at peak-load hour (hour 16) is shown in Figure 8. The results shows that, the voltage profile has been improved through

interaction with DERs, because a portion of the DSLs is supplied locally and the purchased power from the DA market decreases.

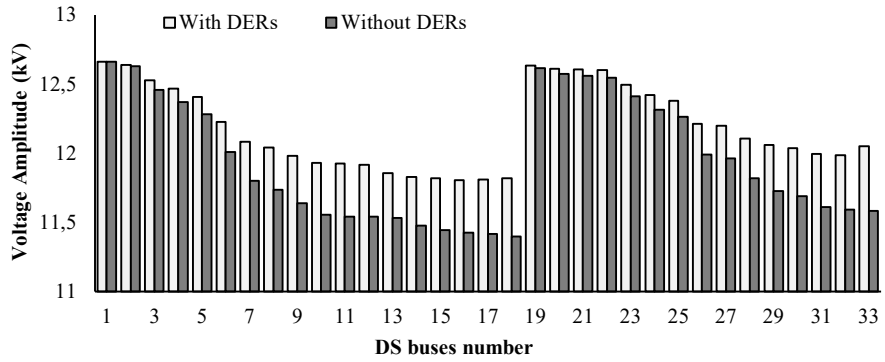

Figure 8. Voltage amplitude of the DS buses at 16th time step in Case I.

4.1.3. Sensitivity Analysis

In this sub-section, sensitivity of the *TC* to the maximum LS factor and the effects of different types of the DERs on the power losses of the DS are investigated.

Let us consider the quantity "minus total cost" as the total benefit, *TB* = -*TC*. Figure 9 reveals that increasing the maximum LS factor makes TB increase, because the amount of DSL decreases at peak-load hours with regard to increasing the amount of DSL that shifts downward. So, the Disco can decrease the purchased power from the DA market with high *MCP*.

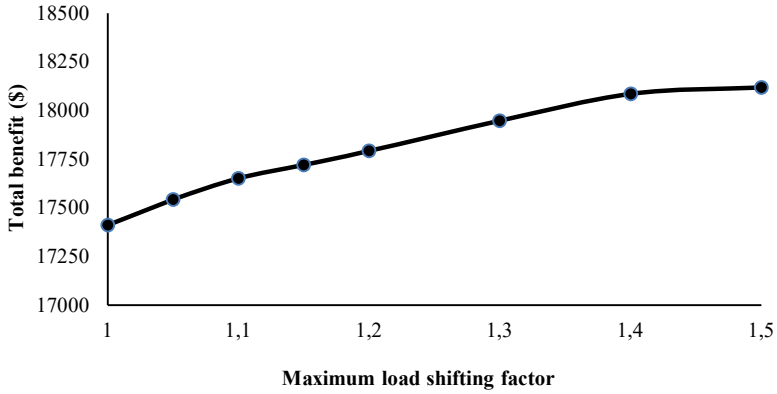

Figure 9. Evolution of the total benefit of the Disco at different maximum LS factors.

In Table 8, the amount of active power losses at each time step according to the various types of DERs in the DS is presented. As shown in this table, DERs have important impact on the amount of power losses at each time step. Modeling the DERs in the decision making problem of the Disco changes the amount of power losses of the DS in a non-negligible way.

Table 8. The amount of power losses considering various types of DERs (MW).

Time (hour)	Without DERs	Types of DERs			
		LS	RES & DG	RES, DG, & IL	RES, DG, & LS
1	0.742	0.950	0.547	0.281	0.735
2	0.660	0.846	0.418	0.141	0.578
3	0.601	0.765	0.341	0.341	0.479
4	0.582	0.739	0.331	0.331	0.466
5	0.606	0.778	0.368	0.368	0.513
6	0.687	0.871	0.395	0.395	0.555
7	0.828	1.060	0.533	0.533	0.730
8	1.028	1.334	0.679	0.679	0.926
9	1.229	1.581	0.373	0.372	0.531
10	1.446	1.802	0.546	0.546	0.625
11	1.649	1.886	0.646	0.646	0.640
12	1.824	1.947	0.730	0.730	0.631
13	1.968	1.942	0.791	0.791	0.628
14	2.063	1.930	0.816	0.816	0.630
15	2.151	0.407	0.894	0.894	0.376
16	2.179	0.412	0.961	0.961	0.364
17	2.126	1.932	0.996	0.996	0.627
18	1.984	1.803	0.848	0.848	0.620
19	1.884	1.788	0.876	0.876	0.640
20	1.833	1.950	0.901	0.901	0.634
21	1.649	2.138	0.767	0.767	1.092
22	1.330	1.716	0.558	0.558	0.804
23	1.027	1.323	0.389	0.437	0.701
24	0.864	1.107	0.665	0.120	0.885
Total power losses	33.012	33.007	15.421	14.328	15.410

4.2. Case II

4.2.1. Input data

The 43-bus real DS connected to the IEEE 24-bus power system is shown in Figure 10. The technical data of this real DS is given in Appendix C. The proportion of each bus's load from the wholesale demand of this DS is given in Appendix C: in this regard, the forecasted DSL in each hour (described in Case I) is divided into the buses of this system. Moreover, the other input data related to the DERs as well as the TS is the same presented in Case I. Also, the location of DERs as well as other technical data are given in Table 9.

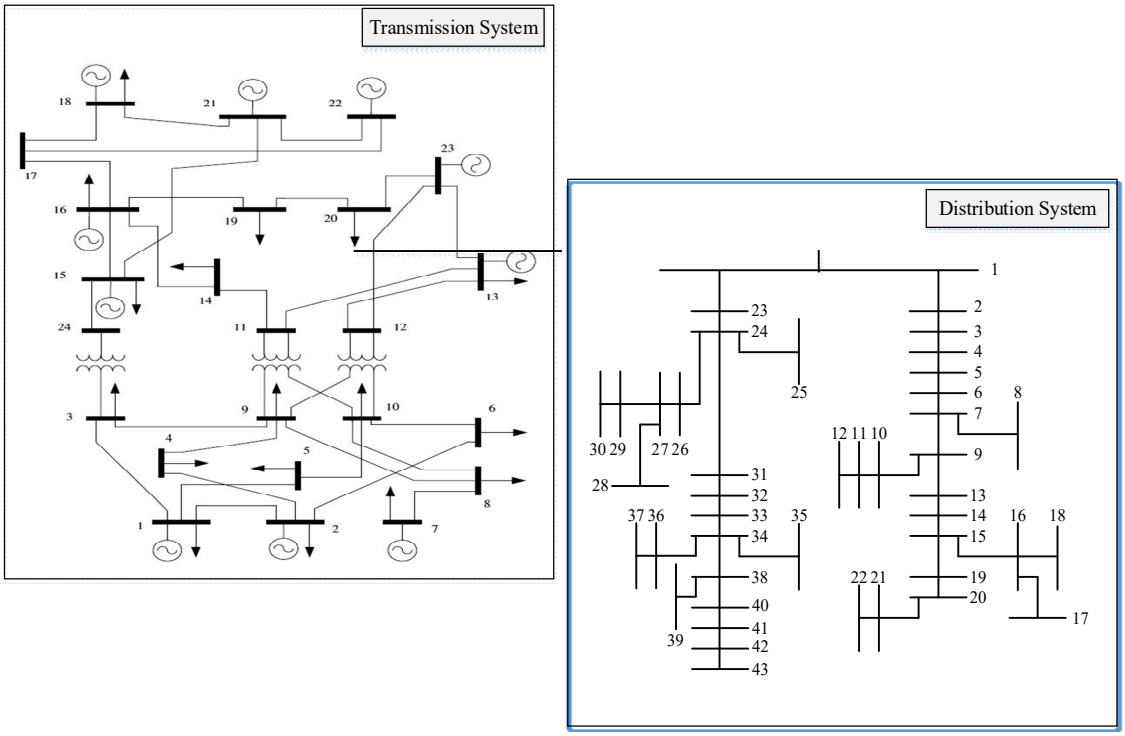

Figure 10. The structure of the 43-bus real DS connected to the 24-bus TS (Case II).

Table 9. DS technical data and DER locations in Case II.

$\bar{P}_{i,j,t}^{\text{flow\_DS}}$ (MW)	$\underline{P}_{i,j,t}^{\text{flow\_DS}}$ (MW)	$\bar{V}_{i,t}^{\text{DS}}$ (p.u.)	$\underline{V}_{i,t}^{\text{DS}}$ (p.u.)	$V_{\text{base}}^{\text{DS}}$ (kV)	Main substation (MVA)
60	-60	1.1	0.9	20.00	80
Type of DER	WT	PV	DG		LS
DS bus location	12, 17, 30, 35	5, 10, 26, 39	8, 22, 37, 43		15-43

4.2.2. Results

The results from applying the proposed model on the real DS are presented in Figures 11-13. The *MCP* and the power balance results of the wholesale market are presented in Figures 11 and 12, respectively. As shown in these Figures, the Disco decreases the purchased power from the market especially at the hours with high energy price through the optimal scheduling of DERs in the DS. This decision of the Disco leads to decreasing the operation cost and the power losses of the DS. As shown in Figures 11 and 12, reducing the amount of the purchased power by the Disco from the market at hours 15-16 and 18-19 leads to changing the *MCPs* from 18.2 $/MWh, 18.2 $/MWh, 18.6 $/MWh, and 18.6 $/MWh to 15.97 $/MWh, 15.97 $/MWh, 18.2 $/MWh, and 18.2 $/MWh, respectively. The Disco's decisions to meet the DNL in this case are shown in Figure 13. The Disco is capable to interact with the DRA as much as possible for providing enough generation with the lower cost instead of trading power with the market at hours 15-16. Also, the Disco uses the power generation capacity provided by all aggregators to decrease its purchased power from the wholesale market at hours 18-19.

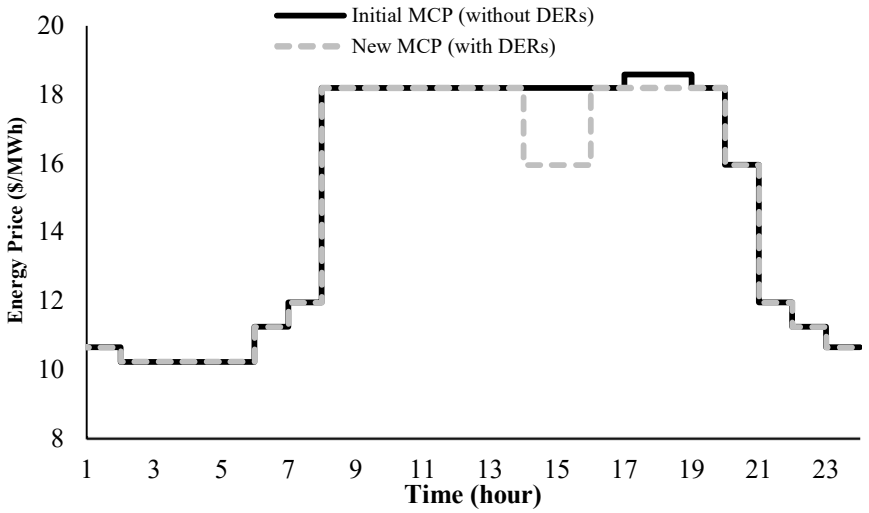

Figure 11. The *MCP* of the DA energy market in Case II.

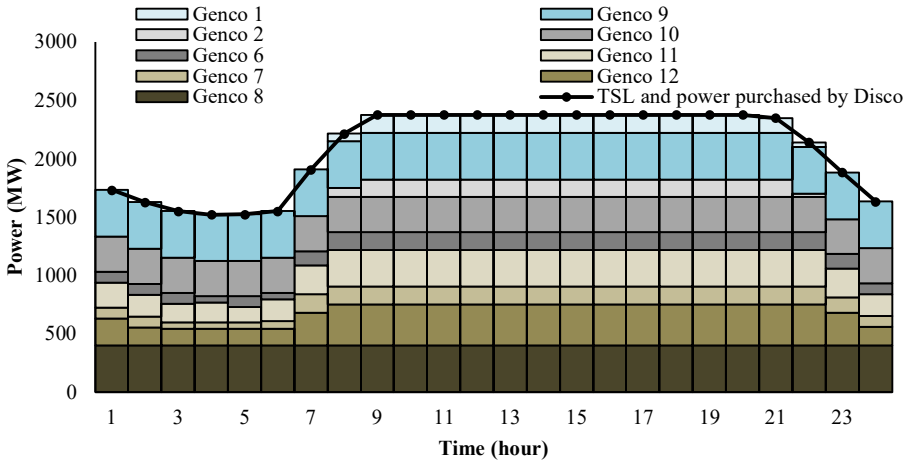

Figure 12. Share of each Genco to meet TSLs and DSL in Case II.

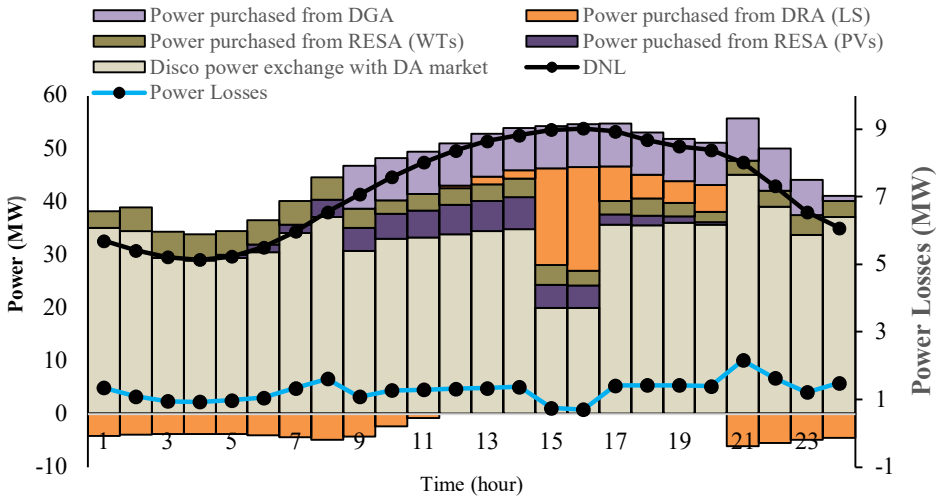

Figure 13. The share of the resources to meet the power balance of the DS in Case II.

4.3. Results for IGDT-based decision-making

In this sub-section, the effect of the uncertainties related to the output power of RESs on the Disco's decisions using the IGDT approach is presented. For this purpose, the objective function of the Disco without considering the IGDT constraints is considered as TC_b (the base case), whereas the IGDT-based optimization model is solved to obtain the robust decision-making of the Disco. The behavior of the risk-averse Disco in Cases I and II is shown in Table 10 and Figure 14 as well as in Table 11 and Figure 15, respectively. As shown in Figures 14(a) and 15(a), the uncertainty radius increases as the risk-aversion parameter increases. In other words, the risk-averse Disco prefers not to employ the RESs as much as possible because of their uncertainty. As a result, the Disco compensates the lack of the generation power of RESs through increasing the DG output power and the purchased power from the market. It is clear that, the mentioned changes in the decision-making of the Disco lead to increasing the TC (decreasing the minus TC). On the other hand, increasing the risk-level of decision-making would also increase the amount of power losses since the purchased power from the market increases (see Figures 14(b) and 15(b)). The sensitivity analysis to the risk-aversion parameter to achieve a more robust results is presented in Tables 10 and 11. It can be seen that, decreasing the amount of RESs output power (increasing the uncertainty radius) changes the interaction with the DGA as well as the wholesale market.

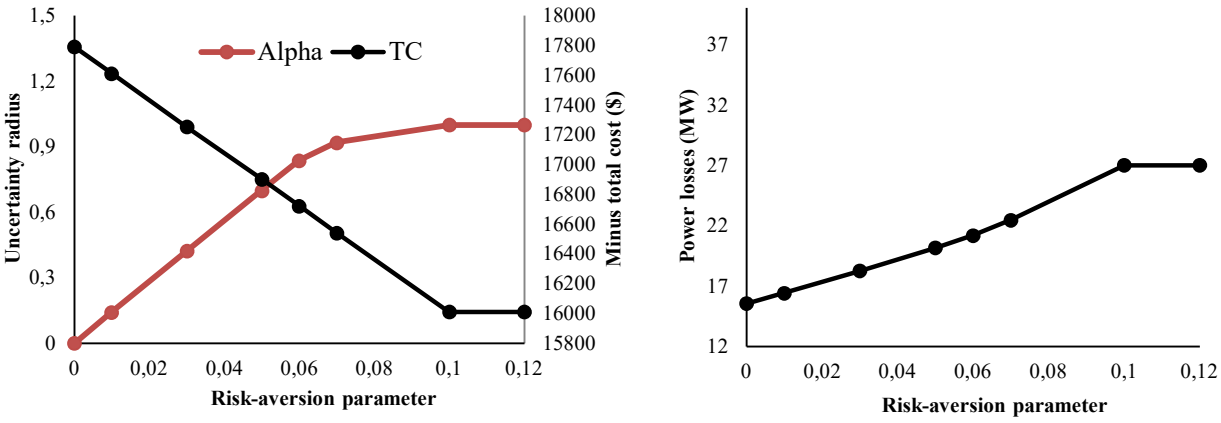

(a) (b)

Figure 14. The sensitivity of TC, uncertainty radius (a), and power losses (b) to risk aversion parameter in Case I

Table 10. The sensitivity of the Disco's decision variables to the risk-aversion parameter in Case I.

Variables	$\zeta = 0$	$\zeta = 0.01$	$\zeta = 0.03$	$\zeta = 0.05$	$\zeta = 0.06$	$\zeta = 0.07$	$\zeta = 0.1$
$\sum_t P_t^{\text{Dis\_DA}}$	781.863	801.736	841.401	873.514	900.045	902.982	968.615
$\sum_t P_t^{\text{DG}}$	116.0	116.0	116.0	116.5	116.628	124.906	84.067
$\sum_t P_t^{\text{WT}}$	71.309	71.309	48.116	24.511	13.641	6.883	0.0
$\sum_t P_t^{\text{PV}}$	52.40	45.042	30.392	16.122	8.579	4.621	0.0

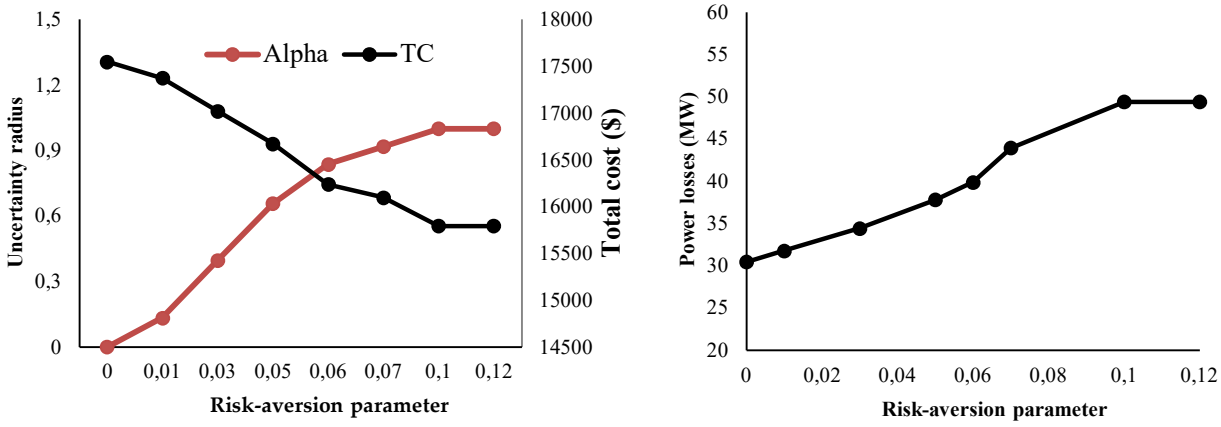

(a) (b)

Figure 15. The sensitivity of TC, uncertainty radius (a), and power losses (b) to the risk aversion parameter in Case II.

Table 11. The sensitivity of Disco's decision variables to the risk-aversion parameter in Case II.

Variables	$\zeta = 0$	$\zeta = 0.01$	$\zeta = 0.03$	$\zeta = 0.05$	$\zeta = 0.06$	$\zeta = 0.07$	$\zeta = 0.1$
$\sum_t P_t^{\text{Dis\_DA}}$	793.354	812.235	849.058	886.424	890.325	896.469	900.045
$\sum_t P_t^{\text{DG}}$	119.607	119.901	121.25	121.968	122.617	125.296	98.142
$\sum_t P_t^{\text{WT}}$	82.96	72.011	50.24	28.639	15.029	8.252	0.0
$\sum_t P_t^{\text{PV}}$	52.40	45.484	31.732	18.089	10.893	5.067	0.0

5. Conclusions

In this paper, the coordination between transmission systems, distribution systems, and DER aggregators is modeled using a local market model. For this purpose, a bi-level optimization approach is proposed, in which the decision-making framework of active distribution systems including Disco and DERs aggregators is modeled as the upper level problem. Moreover, the clearing process of the market by the wholesale market operator is modeled as the lower level problem. The proposed non-linear bi-level model is transformed into a MILP one using KKT conditions and dual theory. The IGDT approach is also used to model the uncertainties of RESs in the decision-making of the Disco. Two cases are defined consisting the IEEE test system and a real DS which both of them connected to the IEEE test power system. To show the effectiveness of the proposed model in this paper, the performance of three decision variables consisting of the *MCP*, the power losses, and the voltage amplitude are investigated. The main conclusions arising from the results regarding these variables are as follows:

- Participating of the Disco in the presence of DERs as a price-maker player in wholesale market decreases the *MCP* since the DERs increases the Disco's ability to influence the *MCP* through presenting bids/offers in the DA market.
- The DS indices consisting of the power losses and the voltage amplitude improve through the optimal decisions of the Disco in this model, i.e., the optimal scheduling of DERs in the LEM and the optimal participation in the wholesale market.
- The various types of DERs and their characteristics change the DS power flow as well as the Disco's behavior for participating in the market. For instance, the results show the difference between Disco's bid in the presence of ILs and LSs.
- The LS cannot decrease the whole amount of power losses significantly. However, the power consumption can be shifted from peak-load hours to other hours. Therefore, the amount of power losses in each hour changes, and could alleviate overloads in the main substation and in DS feeders. Moreover, increasing the capacity of LS related to the DRA is a suitable way to decrease the total cost of DS operation.
- Modeling the DERs in the operation problem of the Disco has the consequence that the Disco can trade energy with the DERs besides the wholesale market to increase its profit.
- With increasing the risk-level of the Disco's decision-making, it increases the purchased power from the wholesale market to manage the uncertainties of RESs which leads to increasing the amount of power losses. This decision is consequently increases the robustness of the decision-making of the Disco.

Acknowledgment

J.P.S. Catalão acknowledges the support by FEDER funds through COMPETE 2020 and by Portuguese funds through FCT, under POCI-01-0145-FEDER-029803 (02/SAICT/2017).

References

[1] G. de Jong, O. Franz, P. Hermans, and M. Lallemand, "TSO-DSO data management report," *TSO-DSO Project Team, Tech. Rep,* 2016.

[2] J. Silva, J. Sumaili, R. J. Bessa, L. Seca, M. A. Matos, V. Miranda*, et al.*, "Estimating the active and reactive power flexibility area at the TSO-DSO interface," *IEEE Transactions on Power Systems,* vol. 33, pp. 4741-4750, 2018.

[3] U. S. E. Framework, "USEF: the framework explained," *Arnhem, The Netherlands,* 2015.

[4] S. o. N. Y. P. S. Commission, "Case 14-M-0101–Proceeding on Motion of the Commission in Regard to Reforming the Energy Vision. Order Adopting Regulatory Policy Framework and Implementation Plan," *February,* vol. 26, p. 11, 2015.

[5] H. Gerard, E. I. R. Puente, and D. Six, "Coordination between transmission and distribution system operators in the electricity sector: A conceptual framework," *Utilities Policy,* vol. 50, pp. 40-48, 2018.

[6] H. Rashidizadeh-Kermani, M. Vahedipour-Dahraie, M. Shafie-khah, and J. P. Catalão, "Stochastic programming model for scheduling demand response aggregators considering uncertain market prices and demands," *International Journal of Electrical Power & Energy Systems,* vol. 113, pp. 528-538, 2019.

[7] İ. Şengör, A. Çiçek, A. K. Erenoğlu, O. Erdinç, and J. P. Catalão, "User-Comfort Oriented Optimal Bidding Strategy of an Electric Vehicle Aggregator in Day-Ahead and Reserve Markets," *International Journal of Electrical Power & Energy Systems,* vol. 122, p. 106194, 2020.

[8] H. Chabok, M. Roustaei, M. Sheikh, and A. Kavousi-Fard, "On the assessment of the impact of a price-maker energy storage unit on the operation of power system: The ISO point of view," *Energy,* vol. 190, p. 116224, 2020.

[9] M. Doostizadeh and H. Ghasemi, "Day-ahead scheduling of an active distribution network considering energy and reserve markets," *International Transactions on Electrical Energy Systems,* vol. 23, pp. 930-945, 2013.

[10] C. Zhang, Q. Wang, J. Wang, P. Pinson, J. M. Morales, and J. Østergaard, "Real-time procurement strategies of a proactive distribution company with aggregator-based demand response," *IEEE Transactions on Smart Grid,* vol. 9, pp. 766-776, 2016.

[11] C. Zhang, Q. Wang, J. Wang, P. Pinson, and J. Østergaard, "Real-time trading strategies of proactive DISCO with heterogeneous DG owners," *IEEE Transactions on Smart Grid,* vol. 9, pp. 1688-1697, 2016.

[12] S. Fan, Q. Ai, and L. Piao, "Bargaining-based cooperative energy trading for distribution company and demand response," *Applied energy,* vol. 226, pp. 469-482, 2018.

[13] S. Wang, K. Wang, F. Teng, G. Strbac, and L. Wu, "An affine arithmetic-based multi-objective optimization method for energy storage systems operating in active distribution networks with uncertainties," *Applied Energy,* vol. 223, pp. 215-228, 2018.

[14] T. Lu, Q. Ai, and Z. Wang, "Interactive game vector: A stochastic operation-based pricing mechanism for smart energy systems with coupled-microgrids," *Applied energy,* vol. 212, pp. 1462-1475, 2018.

[15] S. Bahramara, M. P. Moghaddam, and M. Haghifam, "A bi-level optimization model for operation of distribution networks with micro-grids," *International Journal of Electrical Power & Energy Systems,* vol. 82, pp. 169-178, 2016.

[16] S. Bahramara, M. P. Moghaddam, and M. R. Haghifam, "Modelling hierarchical decision making framework for operation of active distribution grids," *IET Generation, Transmission & Distribution,* vol. 9, pp. 2555-2564, 2015.

[17] S. M. B. Sadati, J. Moshtagh, M. Shafie-khah, A. Rastgou, and J. P. Catalão, "Bi-level model for operational scheduling of a distribution company that supplies electric vehicle parking lots," *Electric Power Systems Research,* vol. 174, p. 105875, 2019.

[18] A. Bostan, M. S. Nazar, M. Shafie-khah, and J. P. Catalão, "Optimal scheduling of distribution systems considering multiple downward energy hubs and demand response programs," *Energy,* vol. 190, p. 116349, 2020.

[19] S. Bahramara, M. Yazdani-Damavandi, J. Contreras, M. Shafie-Khah, and J. P. Catalão, "Modeling the strategic behavior of a distribution company in wholesale energy and reserve markets," *IEEE Transactions on Smart Grid,* vol. 9, pp. 3857-3870, 2018.

[20] A. Papavasiliou, "Analysis of distribution locational marginal prices," *IEEE Transactions on Smart Grid,* vol. 9, pp. 4872-4882, 2017.

[21] E. Mohagheghi, A. Gabash, M. Alramlawi, and P. Li, "Real-time optimal power flow with reactive power dispatch of wind stations using a reconciliation algorithm," *Renewable Energy,* vol. 126, pp. 509-523, 2018.

[22] A. Zecchino, K. Knezović, and M. Marinelli, "Identification of conflicts between transmission and distribution system operators when acquiring ancillary services from electric vehicles," in *2017 IEEE PES Innovative Smart Grid Technologies Conference Europe (ISGT-Europe)*, 2017, pp. 1-6.

[23] A. Papavasiliou and I. Mezghani, "Coordination schemes for the integration of transmission and distribution system operations," in *2018 Power Systems Computation Conference (PSCC)*, 2018, pp. 1-7.

[24] D. S. Stock, F. Sala, A. Berizzi, and L. Hofmann, "Optimal control of wind farms for coordinated TSO-DSO reactive power management," *Energies,* vol. 11, p. 173, 2018.

[25] Z. Mi, Y. Jia, J. Wang, and X. Zheng, "Optimal scheduling strategies of distributed energy storage aggregator in energy and reserve markets considering wind power uncertainties," *Energies,* vol. 11, p. 1242, 2018.

[26] A. Kumar, N. K. Meena, A. R. Singh, Y. Deng, X. He, R. Bansal*, et al.*, "Strategic integration of battery energy storage systems with the provision of distributed ancillary services in active distribution systems," *Applied Energy,* vol. 253, p. 113503, 2019.

[27] M.-E. H.-G. Moossa Khodadadi Arpanahi, "A competitive decentralized framework for Volt-VAr optimization of transmission and distribution systems with high penetration of distributed energy resources," *Electric Power Systems Research,* vol. 186, p. 106421, 2020.

[28] Y. Xie, L. Liu, Q. Wu, and Q. Zhou, "Robust model predictive control based voltage regulation method for a distribution system with renewable energy sources and energy storage systems," *International Journal of Electrical Power & Energy Systems,* vol. 118, p. 105749, 2020.

[29] S. Bahramara, A. Mazza, G. Chicco, M. Shafie-khah, and J. P. S. Catalão, "Comprehensive review on the decision-making frameworks referring to the distribution network operation problem in the presence of distributed energy resources and microgrids," *International Journal of Electrical Power & Energy Systems,* vol. 115, p. 105466, 2020/02/01/ 2020.

[30] P. G. Da Silva, D. Ilić, and S. Karnouskos, "The impact of smart grid prosumer grouping on forecasting accuracy and its benefits for local electricity market trading," *IEEE Transactions on Smart Grid,* vol. 5, pp. 402-410, 2013.

[31] P. Shamsi, H. Xie, A. Longe, and J.-Y. Joo, "Economic dispatch for an agent-based community microgrid," *IEEE Transactions on Smart Grid,* vol. 7, pp. 2317-2324, 2015.

[32] B. A. Bremdal, P. Olivella-Rosell, J. Rajasekharan, and I. Ilieva, "Creating a local energy market," *CIRED-Open Access Proceedings Journal,* vol. 2017, pp. 2649-2652, 2017.

[33] Y. Xiao, X. Wang, P. Pinson, and X. Wang, "A local energy market for electricity and hydrogen," *IEEE Transactions on Power Systems,* vol. 33, pp. 3898-3908, 2017.

[34] S. Park, J. Lee, G. Hwang, and J. K. Choi, "Event-driven energy trading system in microgrids: Aperiodic market model analysis with a game theoretic approach," *IEEE Access,* vol. 5, pp. 26291-26302, 2017.

[35] T. Chen and W. Su, "Local energy trading behavior modeling with deep reinforcement learning," *IEEE Access,* vol. 6, pp. 62806-62814, 2018.

[36] R. Bahmani, H. Karimi, and S. Jadid, "Stochastic electricity market model in networked microgrids considering demand response programs and renewable energy sources," *International Journal of Electrical Power & Energy Systems,* vol. 117, p. 105606, 2020.

[37] N. Rezaei, A. Ahmadi, A. Khazali, and J. Aghaei, "Multiobjective risk-constrained optimal bidding strategy of smart microgrids: An IGDT-based normal boundary intersection approach," *IEEE Transactions on Industrial Informatics,* vol. 15, pp. 1532-1543, 2018.

[38] A. A. Eladl, M. I. El-Afifi, M. A. Saeed, and M. M. El-Saadawi, "Optimal operation of energy hubs integrated with renewable energy sources and storage devices considering CO2 emissions," *International Journal of Electrical Power & Energy Systems,* vol. 117, p. 105719, 2020.

[39] M. J. Rider, J. M. López-Lezama, J. Contreras, and A. Padilha-Feltrin, "Bilevel approach for optimal location and contract pricing of distributed generation in radial distribution systems using mixed-integer linear programming," *IET Generation, Transmission & Distribution,* vol. 7, pp. 724-734, 2013.

[40] A. J. Conejo, M. Carrión, and J. M. Morales, *Decision making under uncertainty in electricity markets* vol. 1: Springer, 2010.

[41] Y. Ben-Haim, *Info-gap decision theory: decisions under severe uncertainty*: Elsevier, 2006.

[42] S. J. Kazempour, A. J. Conejo, and C. Ruiz, "Strategic generation investment using a complementarity approach," *IEEE Transactions on Power Systems,* vol. 26, pp. 940-948, 2010.

[43] S. A. Gabriel, A. J. Conejo, J. D. Fuller, B. F. Hobbs, and C. Ruiz, *Complementarity modeling in energy markets* vol. 180: Springer Science & Business Media, 2012.

Nomenclature

Acronyms

ADS	Active distribution system
DA	Day-ahead
DER	Distributed energy resource
DEMO	Distribution energy market operator
DG	Distributed generation

DGA	Distributed generation aggregator
DR	Demand response
DRA	Demand response aggregator
DS/DSL	Distribution system/Distribution system load
DSM	Demand side management
DSO	Distribution system operator
DSRL/DSNL	Distribution system responsive /non-responsive load
IGDT	Information gap decision theory
IL	Interruptible load
KKT	Karush-Kuhn-Tucker
LEM	Local energy market
LES	Local energy system
LL	Lower level
LS	Load shifting
MCP	Market clearing price
MG	Microgrid
NL	Non-responsive load
PV	Photovoltaic
RES	Renewable energy source
SESP	Smart energy service provider
TB	Total benefit
TC/TC_b	Total cost/Base total cost
TS/TSL	Transmission system/Transmission system load
TSO	Transmission system operator
UL	Upper level
WMO	Wholesale market operator
WT	Wind turbine

Indices

b, B	Index and number of energy and offers/bids block of Gencos/TSLs
$c,\ C$	Index and number of ILs
$e,\ E$	Index and number of LSs
d, D	Index and number of TSLs
$f,\ F$	Index and number of WTs

g, G	Index and number of Gencos
$i,\ I$	Indices and numbers of DS buses
$j,\ J$	Indices and numbers of DS buses
k, K	Index and number of DGs
l, L	Index and number of NLs
n, N	Index and number of TS buses
r, R	Index and number of TS buses
$s,\ S$	Index and number of PV systems
t, T	Index and number of time steps

Sets

$\mathbb{B}_n^{\mathrm{TS}}$	Set of buses directly connected to TS bus *n*
$\mathbb{B}_i^{\mathrm{DS}}$	Set of buses directly connected to DS bus *i*
$\mathbb{M}_n^{\mathrm{G}}/\mathbb{M}_n^{\mathrm{D}}$	Set of Genco/TSL located at bus *n*
$\mathbb{M}_i^{\mathrm{WT}}/\mathbb{M}_i^{\mathrm{PV}}/\mathbb{M}_i^{\mathrm{DG}}$	Set of WT/PV/DG located at bus *i*
$\mathbb{M}_i^{\mathrm{LS}}/\mathbb{M}_i^{\mathrm{IL}}/\mathbb{M}_i^{\mathrm{NL}}$	Set of LS/IL/NL located at bus *i*
$\mathbb{Y}$	Set of the uncertain parameters

Parameters

$B_{(n,r)}$	Susceptance of TS line (*n*,*r*)
$C_{b,g,t}^{\mathrm{TS\_DA}}/C_{b,d,t}^{\mathrm{TS\_DA}}$	Offers/bids block of Genco/TSL ($/MWh)
C_t^{RES}	Operation cost of RES ($/MWh)
d_t	Duration of time step *t* (hour)
$\bar{f}_{(n,r)}^{\mathrm{TS}}$	Capacity limit of TS line (*n*,*r*) (MW)
$\bar{I}_{i,j}^{\mathrm{DS}}$	Upper/Lower limit of DS feeder current (kA)
$\overline{L}_{d,t}^{\mathrm{TS}}/\bar{l}_{b,d,t}^{\mathrm{TS}}$	Max demand/size of TSL energy block (MW)
M	The large amount used for linearizing the equations
$\bar{P}_g/\overline{\rho}_{b,g}^{\mathrm{TS}}$	Max production/size of Genco energy block (MW)
$\overline{P}^{\mathrm{Dis\_TS}}/\underline{P}^{\mathrm{Dis\_TS}}$	Upper / lower limits of power trading limits with the wholesale market (MW)
$P_{e,t}^{\mathrm{DSRL}}/P_{l,t}^{\mathrm{DSNL}}$	Responsive/Non-responsive DSLs (MW)
$\overline{P}_{f,t}^{\mathrm{WT}}/\overline{P}_{s,t}^{\mathrm{PV}}$	Maximum output power of WT / PV (MW)
$\overline{P}_k^{\mathrm{DG}}/\underline{P}_k^{\mathrm{DG}}$	Upper/Lower limit of DG (MW)

$\overline{P}_c^{\mathrm{IL}}$	Maximum amount of interrupted load (MW)
$R_{i,j}^{\mathrm{DS}}$	Resistance of DS line from node *i* to node *j* (Ω)
$\overline{r}_k^{\mathrm{DG}}/\underline{r}_k^{\mathrm{DG}}$	Ramp-up/down limits of DG (MW/h)
$\overline{V}^{\mathrm{DS}}/\underline{V}^{\mathrm{DS}}$	Upper/Lower limit of voltage of DS bus (kV)
$Z_{i,j}^{\mathrm{DS}}$	Impedance of DS line from node *i* to node *j* (Ω)
ζ	Risk-aversion parameter
γ	Generic uncertain parameter
Γ_{LS}	Maximum load shifting
$\lambda_t^{\mathrm{IL}}/\ \lambda_t^{\mathrm{SH}}/\lambda_t^{\mathrm{DG}}$	Offer of DRA/DGA
λ_t^{DSL}	Selling energy price to DSL by the Disco ($/MWh)
ρ_{LS}	Load control factor

Scalar variables

$C_t^{\mathrm{Dis\_DA}}$	Bid/Offer of the Disco in the DA market ($/MWh)
$\boldsymbol{I_{i,j,t}^{\mathrm{DS}}/I_{i,j,t}^{\mathrm{DS\_sqr}}}$	Current magnitude/Linearized DS feeder current from bus *i* to *j* (kA) / $(\mathrm{kA})^2$
$L_{d,t}^{\mathrm{TS}}, l_{b,d,t}^{\mathrm{TS}}$	Amount of TSL and its block (MW)
$\boldsymbol{P_{g,t}^{\mathrm{TS}}, \rho_{b,g,t}^{\mathrm{TS}}}$	Output power of Genco and its block (MW)
$P_t^{\mathrm{Dis\_DA}}$	Disco power exchange with wholesale market (MW)
$\boldsymbol{P_{f,t}^{\mathrm{WT}}/P_{s,t}^{\mathrm{PV}}}$	Output power of RESs (MW)
$P_{k,t}^{\mathrm{DG}}$	Amount of purchased power from DRA (MW)
$P_{c,t}^{\mathrm{IL}}/P_{e,t}^{\mathrm{SH}}$	Amount load interruption/shifting (MW)
$\boldsymbol{P_{i,j,t}^{\mathrm{flow\_DS}}}$	Active power flow from bus *i* to *j* MW)
$P_{i,j,t}^{\mathrm{loss\_DS}}$	Active power losses in the branch from node *i* to node *j* (MW)
$u_{k,t}^{\mathrm{DG}}/u^{\mathrm{Lin}}$	Binary variables
$\boldsymbol{V_{i,t}^{\mathrm{DS}}/\ V_{i,t}^{\mathrm{DS\_sqr}}}$	Voltage/Linearized voltage of DS buses (kV) / $(\mathrm{kV})^2$
$\boldsymbol{\alpha}$	Uncertainty radius
$\boldsymbol{\gamma_{e,t}}$	Load shifting factor
$\boldsymbol{\theta_{n,t}^{\mathrm{TS\_DA}}}$	Voltage angle of TS bus *n* (rad)
$\boldsymbol{\lambda_{n,t}^{\mathrm{TS\_DA}}}$	DA market clearing price ($/MWh)
$\boldsymbol{\lambda, \mu}$	Lagrangian multipliers

Vectors, matrices and general symbols

x	Vector of variables

$f(.)$	Generic objective problem
$\mathbf{g}(.), \mathbf{h}(.)$	Vector of equality and inequality functions
$\boldsymbol{\psi}$	Array of decision variables
$\boldsymbol{\Xi}$	Array of optimization variables
$\mathcal{L}$	Lagrangian function
$\mathcal{U}$	Uncertainty function

Appendix A: Mathematical Program with Equilibrium Constraints (MPEC)

There are some approaches for transforming bi-level optimization models. To make the bi-level problem formulated in a sound way, the UL and LL problems have to be conflicting with each other [40]. If the LL problem is linear (and thus convex), the Karush-Kuhn-Tucker (KKT) conditions can be applied to transform the initial bi-level problem into a single-level problem [43].

In this paper, the Disco bids/offers and the power exchange with the DA market are considered as parameters in the LL problem. Therefore, the LL is linear and convex and can be replaced with the KKT conditions. The KKT conditions consist of four sets of constraints, described as follows.

A.1. Stationarity Constraints

The Lagrangian function ($\mathcal{L}$) is constructed as in Equation (A.1), where $\mathbf{x}$ is the vector of variables of the LL problem, while $f(\mathbf{x})$, $\mathbf{h}(\mathbf{x})$, and $\mathbf{g}(\mathbf{x})$ are the objective function, the equality constraints, and the inequality constraints, respectively. The stationary equations are obtained by derivation from this function for each decision variable as described in (A.2)-(A.7).

$$\mathcal{L}^{\mathrm{DA}} = f(\mathbf{x}) + \boldsymbol{\lambda}^{\mathrm{T}}\mathbf{h}(\mathbf{x}) + \boldsymbol{\mu}^{\mathrm{T}}\mathbf{g}(\mathbf{x}) \tag{A.1}$$

$$\frac{\partial \mathrm{L}^{\mathrm{DA}}}{\partial P_t^{\mathrm{Dis\_DA}}} = -C_t^{\mathrm{Dis\_DA}} + \lambda_{n,t|n=m}^{\mathrm{TS\_DA}} - \underline{\mu}_t^{1\_\mathrm{DA}} + \overline{\mu}_t^{1\_\mathrm{DA}} = 0 \tag{A.2}$$

$$\frac{\partial \mathrm{L}^{\mathrm{DA}}}{\partial P_{g,t}^{\mathrm{TS}}} = -\lambda_{n,t}^{\mathrm{TS\_DA}} - \underline{\mu}_{g,t}^{2\_\mathrm{DA}} + \overline{\mu}_{g,t}^{2\_\mathrm{DA}} + \lambda_{g,t}^{1\_\mathrm{DA}} = 0 \tag{A.3}$$

$$\frac{\partial \mathrm{L}^{\mathrm{DA}}}{\partial \rho_{b,g,t}^{\mathrm{TS}}} = C_{b,g,t}^{\mathrm{TS\_DA}} - \underline{\mu}_{b,g,t}^{3\_\mathrm{DA}} + \overline{\mu}_{b,g,t}^{3\_\mathrm{DA}} - \lambda_{g,t}^{1\_\mathrm{DA}} = 0 \tag{A.4}$$

$$\frac{\partial \mathrm{L}^{\mathrm{DA}}}{\partial L_{d,t}^{\mathrm{TS}}} = \lambda_{n,t|n\neq m}^{\mathrm{TS\_DA}} - \underline{\mu}_{d,t}^{4\_\mathrm{DA}} + \overline{\mu}_{d,t}^{4\_\mathrm{DA}} + \lambda_{d,t}^{2\_\mathrm{DA}} = 0 \tag{A.5}$$

$$\frac{\partial \mathrm{L}^{\mathrm{DA}}}{\partial l_{b,d,t}^{\mathrm{TS}}} = -C_{b,d,t}^{\mathrm{TS\_DA}} - \underline{\mu}_{b,d,t}^{5\_\mathrm{DA}} + \overline{\mu}_{b,d,t}^{9\_\mathrm{DA}} - \lambda_{d,t}^{2\_\mathrm{DA}} = 0 \tag{A.6}$$

$$\frac{\partial \mathrm{L}^{\mathrm{DA}}}{\partial \theta_{n,t}^{\mathrm{TS}}} = \sum_{r\in \mathbf{B}_n^{\mathrm{TS}}} B_{n,r}(\lambda_{n,t}^{\mathrm{TS\_DA}} - \lambda_{r,t}^{\mathrm{TS\_DA}}) + \sum_{r\in \mathbf{B}_n^{\mathrm{TS}}} B_{n,r}(\overline{\mu}_{n,r,t}^{\mathrm{6\_DA}} - \overline{\mu}_{r,n,t}^{\mathrm{6\_DA}}) + \sum_{r\in \mathbf{B}_n^{\mathrm{TS}}} B_{n,r}(\underline{\mu}_{r,n,t}^{\mathrm{6\_DA}} - \underline{\mu}_{n,r,t}^{\mathrm{6\_DA}}) - \underline{\mu}_{n,t}^{\mathrm{7\_DA}} + \overline{\mu}_{n,t}^{\mathrm{7\_DA}} + \lambda_{n,t|n=slack}^{\mathrm{3\_DA}} = 0 \quad \text{(A.7)}$$

A.2. Primal, Dual, and Complementary Constraints

$$0 \le \underline{\mu}_t^{\mathrm{1\_DA}} \perp \left(P_t^{\mathrm{Dis\_DA}} - \underline{P}^{\mathrm{Dis\_TS}}\right) \ge 0 \quad , \quad 0 \le \overline{\mu}_t^{\mathrm{1\_DA}} \perp \left(\overline{P}^{\mathrm{Dis\_TS}} - P_t^{\mathrm{Dis\_DA}}\right) \ge 0 \quad \text{(A.8)}$$

$$0 \le \underline{\mu}_{b,g,t}^{\mathrm{3\_DA}} \perp \left(\rho_{b,g,t}^{\mathrm{TS}} - 0\right) \ge 0 \ , \ 0 \le \overline{\mu}_{b,g,t}^{\mathrm{3\_DA}} \perp \left(\overline{\rho}_{b,g,t}^{\mathrm{TS}} - \rho_{b,g,t}^{\mathrm{TS}}\right) \ge 0 \quad \text{(A.10)}$$

$$0 \le \underline{\mu}_{d,t}^{\mathrm{4\_DA}} \perp \left(L_{d,t}^{\mathrm{TS}}\right) \ge 0 \ , \ 0 \le \overline{\mu}_{d,t}^{\mathrm{4\_DA}} \perp \left(\overline{L}_{d,t}^{\mathrm{TS}} - L_{d,t}^{\mathrm{TS}}\right) \ge 0 \quad \text{(A.11)}$$

$$0 \le \underline{\mu}_{b,d,t}^{\mathrm{5\_DA}} \perp \left(l_{b,d,t}^{\mathrm{TS}} - 0\right) \ge 0 \ , \ 0 \le \overline{\mu}_{b,d,t}^{\mathrm{5\_DA}} \perp \left(\overline{l}_{b,d,t}^{\mathrm{TS}} - l_{b,d,t}^{\mathrm{TS}}\right) \ge 0 \quad \text{(A.12)}$$

$$0 \le \underline{\mu}_{n,r,t}^{\mathrm{6\_DA}} \perp \left(B_{n,r}\left(\theta_{n,t}^{\mathrm{TS\_DA}} - \theta_{r,t}^{\mathrm{TS\_DA}}\right) - \left(-\overline{f}_{n,r}^{\mathrm{TS}}\right)\right) \ge 0 \ , \ 0 \le \overline{\mu}_{n,r,t}^{\mathrm{6\_DA}} \perp \left(\overline{f}_{n,r}^{\mathrm{TS}} - B_{n,r}\left(\theta_{n,t}^{\mathrm{TS\_DA}} - \theta_{r,t}^{\mathrm{TS\_DA}}\right)\right) \ge 0 \quad \text{(A.13)}$$

$$0 \le \underline{\mu}_{n,t}^{\mathrm{7\_DA}} \perp \left(\theta_{n,t}^{\mathrm{TS\_DA}} - (-\pi/2)\right) \ge 0 \ , \ 0 \le \overline{\mu}_{n,t}^{\mathrm{7\_DA}} \perp \left(\pi/2 - \theta_{n,t}^{\mathrm{TS\_DA}}\right) \ge 0 \quad \text{(A.14)}$$

$$\lambda_{n,t}^{\mathrm{TS\_DA}}, \lambda_{g,t}^{\mathrm{1\_DA}}, \lambda_{d,t}^{\mathrm{2\_DA}}, \lambda_{n,t|n=slack}^{\mathrm{3\_DA}} \quad \text{Unrestricted} \quad \text{(A.15)}$$

where each equation is linearized as equation (A.16), in which M_1 and M_2 are values large enough and u^{Lin} is a binary variable.

$$0 \le \mathbf{g(x)} \perp \mu \ge 0 \Rightarrow \mathbf{g(x)} \ge 0 \ , \mu \ge 0 \ , \ \mathbf{g(x)} \le M_1 u^{\mathrm{Lin}} \ , \ \mu \le M_2 \left(1 - u^{\mathrm{Lin}}\right) \quad \text{(A.16)}$$

Appendix B: Linearization

In this appendix, the nonlinear term $\lambda_{m,t}^{\mathrm{TS-DA}} P_t^{\mathrm{Dis-DA}}$ in equation (1) is replaced with linear ones. According to the duality theory, the dual of LL problem is defined as follows [43]:

$$\text{Maximize} \sum_{t=1}^{T} \left[\begin{array}{l} \underline{P}^{\mathrm{Dis\_TS}} \underline{\mu}_t^{\mathrm{1\_DA}} - \overline{P}^{\mathrm{Dis\_TS}} \overline{\mu}_t^{\mathrm{1\_DA}} + \sum_{g=1}^{G} \left(\underline{P}_g \, \underline{\mu}_{g,t}^{\mathrm{2\_DA}} - \overline{P}_g \, \overline{\mu}_{g,t}^{\mathrm{2\_DA}} \right) - \sum_{g=1}^{G} \sum_{b=1}^{B} \overline{\rho}_{b,g,t}^{\mathrm{TS}} \overline{\mu}_{b,g,t}^{\mathrm{3\_DA}} \\ - \sum_{d=1}^{D} \overline{L}_{d,t}^{\mathrm{TS}} \overline{\mu}_{d,t}^{\mathrm{4\_DA}} - \sum_{d=1}^{D} \sum_{b=1}^{B} \overline{l}_{b,d,t}^{\mathrm{TS}} \overline{\mu}_{b,d,t}^{\mathrm{5\_DA}} - \sum_{n=1}^{N} \sum_{r=1}^{R} \left(\overline{f}_{n,r}^{\mathrm{TS}} \underline{\mu}_{n,r,t}^{\mathrm{6\_DA}} + \overline{f}_{n,r}^{\mathrm{TS}} \overline{\mu}_{n,r,t}^{\mathrm{6\_DA}} \right) - \sum_{n=1}^{N} \left(\underline{\mu}_{n,t}^{\mathrm{7\_DA}} + \overline{\mu}_{n,t}^{\mathrm{7\_DA}} \right) \frac{\pi}{2} \end{array} \right] \quad \text{(B.1)}$$

The dual constraints of LL problem are the stationarity constraints illustrated in Appendix A. Based on the strong duality theory, the primal variables are optimal solutions of the primal problem and the dual variables are optimal solutions of the dual problem if the objective functions of the primal and dual problem become equal:

$$\sum_{t=1}^{T} d_t \left[\sum_{g=1}^{G}\sum_{b=1}^{B} C_{b,g,t}^{\text{TS\_DA}} \rho_{b,g,t}^{\text{TS}} - \sum_{d=1}^{D}\sum_{b=1}^{B} C_{b,d,t}^{\text{TS\_DA}} l_{b,d,t}^{\text{TS}} - C_t^{\text{Dis\_DA}} P_t^{\text{Dis\_DA}} \right] =$$

$$\sum_{t=1}^{T} \left[\begin{array}{l} \underline{P}^{\text{Dis\_TS}} \underline{\mu}_t^{\text{1\_DA}} - \overline{P}^{\text{Dis\_TS}} \overline{\mu}_t^{\text{1\_DA}} + \sum_{g=1}^{G} \left(\underline{P_g}\, \underline{\mu}_{g,t}^{\text{2\_DA}} - \overline{P}_g\, \overline{\mu}_{g,t}^{\text{2\_DA}} \right) - \sum_{g=1}^{G}\sum_{b=1}^{B} \overline{\rho}_{b,g,t}^{\text{TS}} \overline{\mu}_{b,g,t}^{\text{3\_DA}} \\ - \sum_{d=1}^{D} \overline{L}_{d,t}^{\text{TS}} \overline{\mu}_{d,t}^{\text{4\_DA}} - \sum_{d=1}^{D}\sum_{b=1}^{B} \overline{l}_{b,d,t}^{\text{TS}} \overline{\mu}_{b,d,t}^{\text{5\_DA}} - \sum_{n=1}^{N}\sum_{r=1}^{R} \left(\overline{f}_{n,r}^{\text{TS}} \underline{\mu}_{n,r,t}^{\text{6\_DA}} + \overline{f}_{n,r}^{\text{TS}} \overline{\mu}_{n,r,t}^{\text{6\_DA}} \right) - \sum_{n=1}^{N} \left(\underline{\mu}_{n,t}^{\text{7\_DA}} + \overline{\mu}_{n,t}^{\text{7\_DA}} \right) \frac{\pi}{2} \end{array} \right] \quad \text{(B.2)}$$

The previous equation can be reformulated as follows:

$$\sum_{t=1}^{T} d_t \left(C_t^{\text{Dis\_DA}} P_t^{\text{Dis\_DA}} \right) = \sum_{t=1}^{T} d_t \left[\sum_{g=1}^{G}\sum_{b=1}^{B} C_{b,g,t}^{\text{TS\_DA}} \rho_{b,g,t}^{\text{TS}} - \sum_{d=1}^{D}\sum_{b=1}^{B} C_{b,d,t}^{\text{TS\_DA}} l_{b,d,t}^{\text{TS}} \right] -$$

$$\sum_{t=1}^{T} \left[\begin{array}{l} \underline{P}^{\text{Dis\_TS}} \underline{\mu}_t^{\text{1\_DA}} - \overline{P}^{\text{Dis\_TS}} \overline{\mu}_t^{\text{1\_DA}} + \sum_{g=1}^{G} \left(\underline{P_g}\, \underline{\mu}_{g,t}^{\text{2\_DA}} - \overline{P}_g\, \overline{\mu}_{g,t}^{\text{2\_DA}} \right) - \sum_{g=1}^{G}\sum_{b=1}^{B} \overline{\rho}_{b,g,t}^{\text{TS}} \overline{\mu}_{b,g,t}^{\text{3\_DA}} \\ - \sum_{d=1}^{D} \overline{L}_{d,t}^{\text{TS}} \overline{\mu}_{d,t}^{\text{4\_DA}} - \sum_{d=1}^{D}\sum_{b=1}^{B} \overline{l}_{b,d,t}^{\text{TS}} \overline{\mu}_{b,d,t}^{\text{5\_DA}} - \sum_{n=1}^{N}\sum_{r=1}^{R} \left(\overline{f}_{n,r}^{\text{TS}} \underline{\mu}_{n,r,t}^{\text{6\_DA}} + \overline{f}_{n,r}^{\text{TS}} \overline{\mu}_{n,r,t}^{\text{6\_DA}} \right) - \sum_{n=1}^{N} \left(\underline{\mu}_{n,t}^{\text{7\_DA}} + \overline{\mu}_{n,t}^{\text{7\_DA}} \right) \frac{\pi}{2} \end{array} \right] \quad \text{(B.3)}$$

To achieve the expression of $\lambda_{m,t}^{\text{TS\_DA}} P_t^{\text{Dis\_DA}}$ from $C_t^{\text{Dis\_DA}} P_t^{\text{Dis\_DA}}$, the following approach is applied:

$$\begin{array}{l} \dfrac{\partial \text{L}^{\text{DA}}}{\partial P_t^{\text{Dis\_DA}}} = -C_t^{\text{Dis\_DA}} + \lambda_{m,t}^{\text{TS\_DA}} - \underline{\mu}_t^{\text{1\_DA}} + \overline{\mu}_t^{\text{1\_DA}} = 0 \\ \overline{\mu}_t^{\text{1\_DA}} * \left(\overline{P}^{\text{Dis\_TS}} - P_t^{\text{Dis\_DA}} \right) = 0 \quad \rightarrow \quad \overline{\mu}_t^{\text{1\_DA}} \overline{P}^{\text{Dis\_TS}} = \overline{\mu}_t^{\text{1\_DA}} P_t^{\text{Dis\_DA}} \\ \underline{\mu}_t^{\text{1\_DA}} * \left(P_t^{\text{Dis\_DA}} - \underline{P}^{\text{Dis\_TS}} \right) = 0 \quad \rightarrow \quad \underline{\mu}_t^{\text{1\_DA}} \underline{P}^{\text{Dis\_TS}} = \underline{\mu}_t^{\text{1\_DA}} P_t^{\text{Dis\_DA}} \\ \Rightarrow C_t^{\text{Dis\_DA}} P_t^{\text{Dis\_DA}} = \lambda_{m,t}^{\text{TS\_DA}} P_t^{\text{Dis\_DA}} - \underline{\mu}_t^{\text{1\_DA}} \underline{P}^{\text{Dis\_TS}} + \overline{\mu}_t^{\text{1\_DA}} \overline{P}^{\text{Dis\_TS}} \end{array} \quad \text{(B.4)}$$

The nonlinear expression $\lambda_{m,t}^{\text{TS\_DA}} P_t^{\text{Dis\_DA}}$ is transformed into a linear one as follows:

$$\sum_{t=1}^{T} \lambda_{m,t}^{\text{TS\_DA}} P_t^{\text{Dis\_DA}} = \sum_{t=1}^{T} d_t \left[\sum_{g=1}^{G}\sum_{b=1}^{B} C_{b,g,t}^{\text{TS\_DA}} \rho_{b,g,t}^{\text{TS}} - \sum_{d=1}^{D}\sum_{b=1}^{B} C_{b,d,t}^{\text{TS\_DA}} l_{b,d,t}^{\text{TS}} \right] -$$

$$\sum_{t=1}^{T} \left[\begin{array}{l} \sum_{g=1}^{G} \left(\underline{P_g}\, \underline{\mu}_{g,t}^{\text{2\_DA}} - \overline{P}_g\, \overline{\mu}_{g,t}^{\text{2\_DA}} \right) - \sum_{g=1}^{G}\sum_{b=1}^{B} \overline{\rho}_{b,g,t}^{\text{TS}} \overline{\mu}_{b,g,t}^{\text{3\_DA}} - \sum_{d=1}^{D} \overline{L}_{d,t}^{\text{TS}} \overline{\mu}_{d,t}^{\text{4\_DA}} - \\ \sum_{d=1}^{D}\sum_{b=1}^{B} \overline{l}_{b,d,t}^{\text{TS}} \overline{\mu}_{b,d,t}^{\text{5\_DA}} - \sum_{n=1}^{N}\sum_{r=1}^{R} \left(\overline{f}_{n,r}^{\text{TS}} \underline{\mu}_{n,r,t}^{\text{6\_DA}} + \overline{f}_{n,r}^{\text{TS}} \overline{\mu}_{n,r,t}^{\text{6\_DA}} \right) - \sum_{n=1}^{N} \left(\underline{\mu}_{n,t}^{\text{7\_DA}} + \overline{\mu}_{n,t}^{\text{7\_DA}} \right) \frac{\pi}{2} \end{array} \right] \quad \text{(B.5)}$$

Appendix C: The required technical data for the 43-bus real DS

The amount of the resistance and the impedance of the real DS's lines required for the power flow problem are given in Table C.1. Also the proportion of each bus's load from the whole demand of the DS is presented in Table C.2.

Table C.1. The line data including resistance and impedance for the real DS

# Lines	Lines	*R* (Ω)	*Z* (Ω)	# Lines	Lines	*R* (Ω)	*Z* (Ω)
1	1-2	0.2120	0.3484	22	1-23	0.1187	0.1951
2	2-3	0.0204	0.0336	23	23-24	0.1333	0.2191
3	3-4	0.0132	0.0218	24	24-25	0.1032	0.1697
4	4-5	0.0475	0.0780	25	24-26	0.1110	0.1824
5	5-6	0.1642	0.2699	26	26-27	0.1791	0.2944
6	6-7	0.0505	0.0830	27	27-28	0.0235	0.0386
7	7-8	0.1598	0.2627	28	27-29	0.0533	0.0876
8	7-9	0.2186	0.3593	29	29-30	0.0599	0.0984
9	9-10	0.0726	0.1193	30	24-31	0.2904	0.4772
10	10-11	0.0340	0.0558	31	31-32	0.1220	0.2005
11	11-12	0.0668	0.1098	32	32-33	0.0596	0.0980
12	9-13	0.1281	0.2105	33	33-34	0.1129	0.1855
13	13-14	0.0720	0.1184	34	34-35	0.0522	0.0857
14	14-15	0.0916	0.1506	35	34-36	0.1253	0.2060
15	15-16	0.0883	0.1452	36	36-37	0.0326	0.0535
16	16-17	0.0709	0.1166	37	34-38	0.1369	0.2250
17	16-18	0.0480	0.0789	38	38-39	0.0486	0.0798
18	15-19	0.0466	0.0767	39	38-40	0.0204	0.0336
19	19-20	0.0980	0.1610	40	40-41	0.0513	0.0844
20	20-21	0.0491	0.0807	41	41-42	0.0315	0.0517
21	21-22	0.1099	0.1805	42	42-43	0.0751	0.1234

Table C.2. The proportion of each bus's load from the total DSL

# Load	% of Total DSL	# Load	% of Total DSL
1	0.38	22	1.71
2	0.18	23	2.69
3	1.18	24	1.92
4	2.95	25	1.84
5	1.47	26	1.47
6	1.84	27	1.37
7	1.92	28	1.37
8	4.64	29	1.71
9	3.67	30	2.31
10	2.31	31	2.31
11	4.29	32	4.29
12	2.14	33	2.31
13	8.57	34	3.67
14	2.69	35	2.69
15	1.92	36	1.92
16	1.23	37	1.92
17	1.53	38	1.18
18	1.53	39	3.06
19	3.67	40	1.92
20	2.94	41	1.92
21	2.31	42	3.06